Marine aerosol distributions from shipborne observations over the South China Sea: Diurnal variation characteristics and their controlling factors

Zhi Qiao[1,2,3], Shengcheng Cui[1,3,4,*], Huiqiang Xu[1,2,3], Xiaoqing Wu[1,3,4], Xiaodan Liu[1,2,3], Zihan Zhang[1,4], Mengying Zhai[1,2,3], Yue Pan[5], Tao Luo[1,4], Xuebin Li[1,4]

[1]Key Laboratory of Atmospheric Optics, Anhui Institute of Optics and Fine Mechanics, HFIPS, Chinese Academy of Sciences, Hefei 230031, China
[2]Science Island Branch of Graduate School, University of Science and Technology of China, Hefei 230026, China
[3]Nanhu Laser Laboratory, National University of Defense Technology, Changsha 410073, China
[4]Advanced Laser Technology Laboratory of Anhui Province, Hefei 230037, China
[5] School of Electronic Engineering, Chaohu University, Chaohu, 238024, China

Correspondence to: Shengcheng Cui(csc@aiofm.ac.cn)

Abstract. Marine aerosols critically influence Earth's radiation budget and climate dynamics through their spatial distributions and components due to their ~~generation~~production and transport processes. However, in-situ observational datasets remain limited, particularly in the South China Sea (SCS). Based on our comprehensive shipborne measurements, this study presents a quantitative analysis of marine aerosol distributions and compositional variations between the offshore and pelagic regions ~~environments~~ over the SCS. Our data demonstrate a 120% increase~~elevation~~ in offshore aerosol number concentrations (NCs, $Dp < 10.37$ μm) relative to pelagic baselines, featuring 120% higher accumulation-mode particles ($Dp \leq 1.981$ μm) and 70% higher coarse-mode particles (1.981 μm $< Dp < 10.37$ μm), quantitatively confirming continental transport affects spatial distribution of marine aerosols~~offshore aerosol signatures~~. In contrast, in the pelagic ~~area~~regions, marine aerosols are virtually unaffected by continental source~~transport~~ and distinctly represent characteristics of the local ~~generation~~production. Meteorological analyses identified wind speed (WS) and sea surface temperature (SST) as primary regulators of NC. However, observed NC variations at fixed WS and SST values suggest additional controlling factors. We demonstrate that sea-air temperature differentials (SST-T_{2m}) exhibit a stronger correlation ($r = -0.82$, $p \leq 0.01$) with NC than the other meteorological parameters, where increased SST-T_{2m} ~~corresponded~~led to decreased marine aerosol production. This temperature gradient effect drives pronounced diurnal NC variations, with maximum differences of 35% observed between daytime, nighttime, and transition periods. These findings provide concrete evidence for the spatial and diurnal variability in marine aerosol distributions over the SCS, thereby further improving understanding of marine aerosol transport and production.~~These results prove the key explanations for the variations of spatial and diurnal distributions of marine aerosols to understand marine aerosol generation and transport better.~~

Graphical Abstract

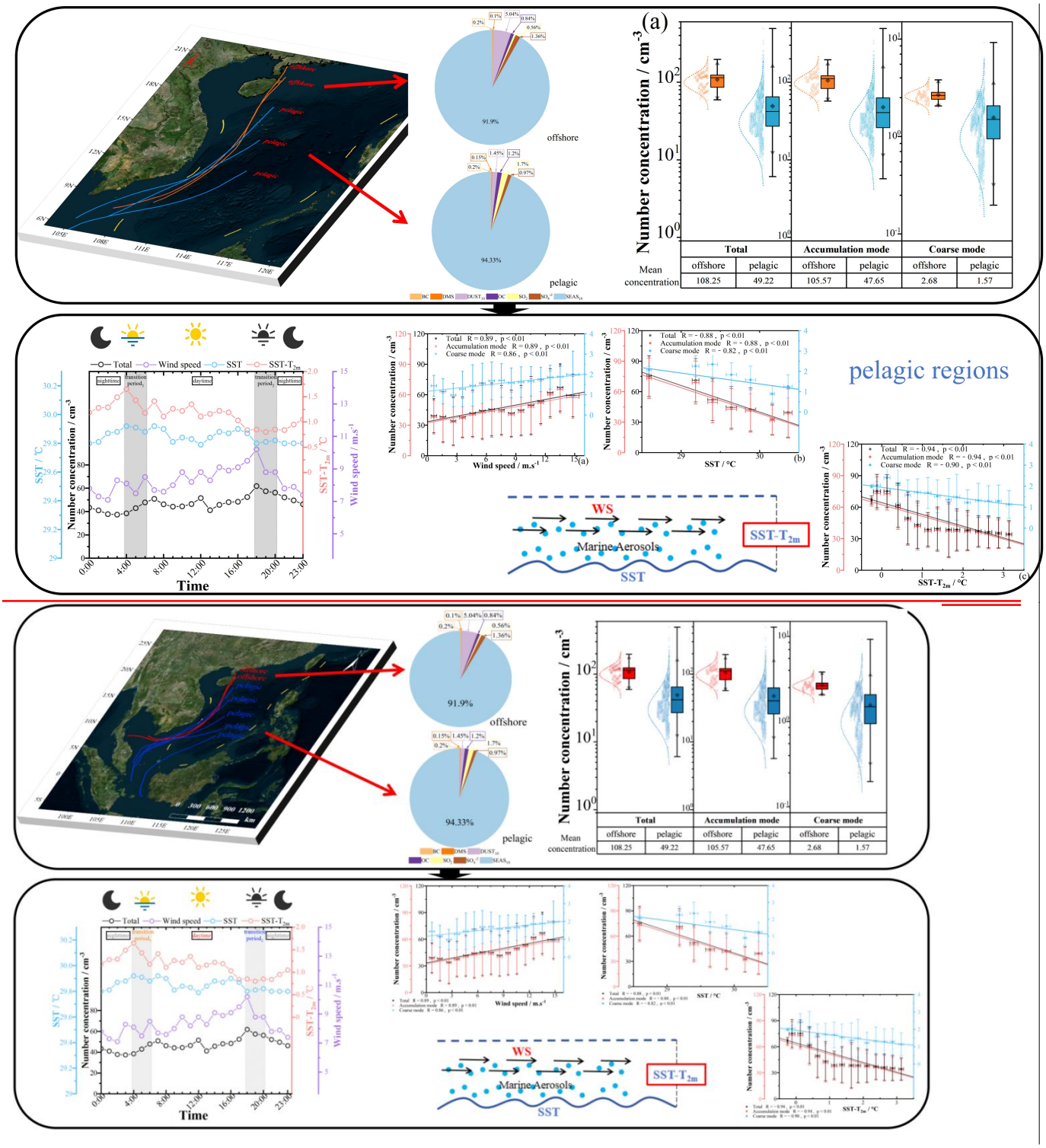

Keywords: Shipborne observation; marine aerosol distributions; aerosol ~~generation~~production and transport; sea-air temperature differences; the South China Sea

1. Introduction

Atmospheric aerosols represent one of the largest uncertainties in the climate system projections for ~~the~~ past and ~~the~~ future (Andreae & Rosenfeld, 2008; Bauer et al., 2020; Bzdek et al., 2020). The ocean covers more than two-thirds of Earth's surface; marine aerosols are generated from the ocean surface and ~~the~~ gas-to-particle conversion in the atmosphere (Korhonen et al., 2008). Globally, they are estimated to account for the largest proportion of ~~the~~ natural aerosol emissions (Nguyen et al., 2017; Textor et al., 2006). Therefore, they represent an essential component of ~~the~~ atmospheric aerosols. ~~Meanwhile, m~~Marine aerosols are divided into two types: anthropogenic aerosols and natural aerosols. The natural category primarily includes sea salt particles and sea spray aerosols (Dedrick et al., 2022; Duce et al., 1965; Sander et al., 2003; Troitskaya et al., 2018). These aerosols modulate the radiative properties by influencing the indirect and direct radiation budget (Decesari et al., 2011; Myhre et al., 2004; Woods et al., 2010). Additionally, they affect the nature of the marine cloud microphysics and precipitation patterns (Feingold et al., 1999; Levin et al., 2005; Woodcock, 1952, 1953) and drive the geochemical cycles at the ocean surface (Alexander et al., 2005; Eriksson, 1960; Lawler et al., 2011; Long et al., 2014). As the essential aerosol type in the atmosphere, marine aerosols play a non-negligible role in the radiation budget. Thus, the role of marine aerosols in the climate system can not be ignored (Li et al., 2022; Meinrat & Paul, 1997).

Due to their non-negligible influence on both radiation budget and climate change, there has been an increasing research focus on marine aerosols over the last~~more and more research on marine aerosols has been conducted for~~ forty years. Early observations by ~~Hoppel (1979, 1985) studied the aerosol NC and the particle size distribution on the east coast of the United States, and the significant changes in the particle size distribution can be associated with the changes in meteorological parameters and oceanic air mass. In addition,~~ Prospero (1979) across multiple marine areas showed notable variations in marine aerosol concentrations, ~~comprehensively reported the mineral and sea salt aerosol concentrations in several marine areas and found that the aerosol mass concentrations from one marine area to the other were relatively different,~~ ranging from 3.34 to 8.71 μg m^{-3}. Subsequent reported measured data verify substantial regional marine aerosol concentration differences between different ocean areas. In polar regions, submicrometer aerosol (Dp ≤ 1000 nm) mass concentrations averaged 0.76 μg m^{-3} in the Arctic (Leck & Persson, 1996) versus 3.15 μg m^{-3} in the Antarctic (Savoie et al., 1993). In the Pacific Ocean, the $PM_{2.5}$ (Dp ≤ 2500 nm) concentration averaged 12.3 ± 9.1 μg m^{-3} in the Western Pacific (Ma et al., 2022) versus 140 ± 48.1 μg m^{-3} in the Bohai Sea (Han et al., 2019). In the Indian Ocean, Pant et al. (2009) observed that the average micrometer aerosols (500 nm ≤ Dp ≤ 10000 nm) mass concentrations were 8.89 μg m^{-3}. ~~In the Arctic, Leck (1996) reported that the submicrometer aerosol (Dp ≤ 1000 nm) mass concentrations during the International Arctic Ocean Expedition (IAOE-91) cruise; for instance, the average mass concentration was 0.76 μ g m^{-3} over the ocean. In terms of the Antarctic, Savoie (1993) reported the submicrometer aerosol (Dp ≤ 1000 nm) concentrations, and the mean concentrations~~

~~were 3.15 μ g m^{-3} at Marsh. Subsequently, Sakerin (2015) measured the marine aerosol (0.3 μm ≤ Dp ≤ 10 μm), and he found that the average mass concentration was 875 ng m^{-3} at the Chukchi and East Siberian seas. In the Indian Ocean, Pant (2009) observed that the average micrometer aerosols (0.5 μm ≤ Dp ≤ 10 μm) mass concentrations were 8.89 μg m^{-3}. For the China waters,~~ In addition to aerosol mass concentrations, researchers have also observed aerosol number concentrations (NCs) differences. For instance, in marine regions off the coast of China, Kim et al. (2009) found that the average submicrometer aerosol particle (10 nm ≤ Dp ≤ 300 nm) concentrations were 4335 ± 2736 cm^{-3}~~m^{-3}~~ over the East China Sea and 5972 ± 2736 cm^{-3} over the Yellow Sea. ~~Han (2019) found that the daily average $PM_{2.5}$ (Dp ≤ 2500 nm) concentration was 140 ± 48.1 μg m^{-3} in the Bohai Sea. All in all~~In summary, there ~~were~~are ~~some discrepancies~~differences in ~~the~~ marine aerosol mass concentrations and NCs~~size distributions~~ between the different ocean areas. However, most available marine aerosol data for the SCS come from coastal monitoring stations, while shipboard observations remain sparse and outdated (Kong et al., 2016; Su et al., 2022). Given that shipboard measurements can provide better spatial and temporal context for marine aerosol measurements across diverse ocean areas such as the SCS, expanding and updating such shipboard observations have the potential to improve the characterization of marine aerosol in these regions.~~; however, there were very few studies of the marine aerosol concentration and particle size distribution in the SCS, especially from 10° N-20° N (Kong et al., 2016; Ma et al., 2022; Su et al., 2022). Most measurement data were observed by the coastal monitoring station, and the shipboard observations are still very sparse in the SCS; moreover, the major measurement data are relatively outdated and need to be updated.~~

~~The a~~Aerosol transport ~~generation~~ and production ~~transport radically~~can ~~led~~lead to the differences in marine aerosol concentration and size distribution. Some studies revealed that marine aerosol components (e.g. sea salt, dust, sulfate, organic carbon) and particle size distribution ~~were~~are influenced by both the occurrence of mesoscale weather events (e.g. thunderstorm, sea breeze, typhoon) and ~~the distance from the coast, and~~continental ~~the aerosol~~ transport ~~was associated with the distances~~ (Athanasopoulou et al., 2016; Chen et al., 2018; Croft et al., 2021; O'Dowd & De Leeuw, 2007; Savoie et al., 2015; Sellegri et al., 2006). As one of the largest marginal seas, the SCS is located on the continental margin and separated from the open ocean by islands, or island arcs. It is significantly influenced by continental and anthropogenic aerosols transported through continental air masses. Previous studies reveal that continental and anthropogenic aerosols play an important role in determining aerosol concentration and size distribution (Braun et al., 2020; Wu & Boor, 2021). Liang et al. (2021) observed the increasing submicron aerosol NCs and different number size distribution shape (20 nm ≤ Dp ≤ 400 nm) when observational data were influenced by continental transport in the SCS. Atwood et al. (2017) further found that under continental transport, the number size distribution exhibits a unimodal structure (20 nm ≤ Dp ≤ 500 nm). In contrast, a distinct bimodal size distribution (20 nm ≤ Dp ≤ 500 nm) emerges without continental transport. Due to limited observational data and the fact that previous studies focused on the submicron size range, conducting observational studies of the impact of aerosol transport on larger aerosol particles (Dp ≥ 500 nm) is crucial for gaining a more thorough comprehension of how aerosol transport influences size distributions.

Furthermore, some key meteorological parameters of the air-sea interface could affect ~~the~~ aerosol ~~generation~~production and

transport, such as wind direction (WD) and speed (WS), relative humidity (RH), and sea surface temperature (SST)~~SST, wind direction (WD) and speed (WS), relative humidity (RH), et al.~~ (Dasarathy et al., 2023; Carslaw et al., 2010; Hoppel, 1979, 1985). ~~Tang (1997) found that the marine aerosol deliquescence (process of the water absorption till they were fully dissolved) and the efflorescence (process of drying until they returned to the crystalline structure) can be associated with the RH values. Therefore, the RH was one of the major factors affecting the marine aerosol concentration and particle size distribution by influencing the aerosol wet deposition and dispersion (Irshad et al., 2009; Wise et al., 2009; Zeng et al., 2013). Meanwhile, p~~Previous studies found that WS is~~was~~ the major driver of ~~the~~ production and transport of marine aerosols. Some subsequent studies attempted to link ~~the~~ NCs to ~~the~~ observed WS (Andreas, 1998, 2010; Gong, 2003; Ovadnevaite et al., 2014; Smith et al., 1993; Yang et al., 2019). These studies derived source functions based on the relationship between aerosol particle size distribution and WS, thereby enabling the simulation of number size distribution and total aerosol NCs. Some studies revealed that rising RH increases particle dry deposition rates (Arimoto & Duce, 1986; Lo et al., 1999), which are important to aerosol transport, as higher dry deposition rates reduce the residence time of aerosols in the atmosphere and shorten their transport distance therein. Ding et al. (2021) found that elevated RH enhances secondary aerosol (e.g. nitrate and sulfate) formation, which directly affects aerosol production. Therefore, RH also affects aerosol transport and production. In addition, SST dramatically influences the production of marine aerosols by affecting bubble bursting time and jet drop production efficiency (Zábori et al., 2012a). Jaeglé et al. (2011) and Mårtensson et al. (2003) further revealed that warmer SST might reduce seawater density and surface tension, ultimately leading to higher marine aerosol production. The reduced surface tension increases wave breaking efficiency, entraining more air into seawater to form bubbles. In addition, the reduced seawater density leads to more bubbles rising back to the sea surface. As these bubbles reach the surface and burst, they subsequently form marine aerosols. ~~and created the generation functions simulating the concentrations by using the relationships (Andreas, 1998, 2002, 2010; Ovadnevaite et al., 2014; Smith et al., 1993). In addition, the SST dramatically influences the production of marine aerosols. They explained that the SST affected the sea surface water density, tension, and so on, all of which affected the bubble formation and bursting process and influenced the production of marine aerosols ultimately (Jaeglé et al., 2011; Mårtensson et al., 2003; Zábori et al., 2012a). As aforementioned, changes in the offshore distances and these meteorological parameters will influence marine aerosol NC and particle size distribution.~~ However, previous studies indicated that sea-air temperature differentials (SST-T_{2m})~~SST-T_{2m}~~ influence~~s~~ the air-sea interaction through air-sea heat exchanges and turbulent mixing (O'Neill et al., 2010); meanwhile, it can comprehensively reflect the characteristics of the ocean and atmosphere near the sea surface (Jing et al., 2019; Ma et al., 2016~~; O'Neill et al., 2010~~). Hence, SST-T_{2m} might affect marine aerosol ~~generation~~production and transport, but the exact effects of SST-T_{2m} on marine aerosols need further investigation. ~~For~~To better quantify~~ing~~ and understand~~ing~~ the effect of these meteorological parameters~~factors~~ on marine aerosols, more thorough information about the variations of marine aerosol and these factors, especially regarding~~for~~ SST-T_{2m}, is~~was~~ needed in the SCS. In addition, the diurnal scale of marine aerosol variation can provide valuable information about their production and transport (Flores et al., 2021), and how these processes are influenced by meteorological parameters. Understanding the diurnal variation is also crucial for improving atmospheric

models. Studies on the scale of diurnal variation in marine aerosol remain scarce, and there is an urgent need to clarify the specific connection between these diurnal variation and meteorological parameters to better understand aerosol production and transport.

~~In summary, most observation data of the marine aerosols and the meteorological parameters were relatively outdated in the SCS; the subsequent updates simultaneously were lacking. Meanwhile, there was a probable relationship between meteorological element change and marine aerosol. Notably, meteorological parameters exhibited significant variations within and between different oceanic regions in terms of the primary factors influencing aerosol generation and transport, implying that the responses of marine aerosol distributions to changes in meteorological parameters could also vary among these areas. Moreover, there was a lack of studies on the scale of the diurnal changes in marine aerosol distributions, and an urgent need for their specific connection to meteorological parameters and distance from the coast to understand aerosol generation and transport better.~~ To address these, we acquired and updated ~~the~~ observations of marine aerosol and meteorological parameters over the SCS, then quantitatively compared ~~the~~ marine aerosol components ~~distributions~~ and distributions ~~components~~ in the offshore and pelagic ~~environments~~regions ~~over the SCS~~, as well as ~~the~~ influence of aerosol transport on marine aerosol. ~~Afterward~~Subsequently, ~~the~~ temporal variations of ~~the~~ shipborne observational~~ed~~ data were investigated in detail; meanwhile, the discrepancies in ~~the~~ distribution of ~~the~~ marine aerosol in ~~the~~ diurnal variations, especially the diurnal transition, were further analyzed. ~~According to~~Based on these analyses, ~~the~~ specific relationships between ~~the~~ different meteorological parameters and marine aerosols were examined ~~respectively~~.; F~~f~~inally, ~~the~~ overall results of marine aerosol particle size distributions and NCs in the SCS, as well as ~~and~~ the possible influence factors were ~~given~~summarized.

2. Cruise observation and data analysis

2.1. Cruise details

In May and June 2023, a scientific cruise was conducted in the SCS by the South China Sea Institute of Oceanology, Chinese Academy of Sciences, ~~carried out a science cruise program in the SCS~~ onboard *Yuezhanyuke N~~O~~0. 6*. This study analyzes the aerosol-meteorology (AM) measurements along the section from the latitude 21°02′ N to 8°5′ N and the longitude 110°33′ E to 115°25′ E. All ~~the~~ AM data were collected from 21 May to 15 June 2023.

2.2. Instrument setup

2.2.1. Aerosol sampling instrument

The NCs of aerosol particles were measured with the Model 3321 Aerodynamic Particle Size (APS) spectrometer (TSI Incorporated, USA), which has 52 size channels in ~~the~~ 0.5 to 20 μm range. This Model 3321 APS spectrometer employs relative light-scattering intensity along with sophisticated time-of-flight techniques; ~~the~~ two complementary techniques can

measure the information of each aerosol particle to obtain ~~the~~ aerosol concentrations and distributions. We used the Particle Loss Calculator (PLC) to calculate particle losses for the APS in this cruise (Fig. S1) (Von Der Weiden et al., 2009). Fig. S1 revealed a dramatic increase in aerosol particle loss at particle diameters exceeding 10 μm. Meanwhile, t~~T~~he accuracy of ~~the~~ aerosol data for particle diameters between 0.5 μm and 10 μm, as measured by the ~~Model 3321~~ APS ~~spectrometer~~, had been fully validated in previous studies (Pagels et al., 2005; Peters et al., 2003; Peters, 2006). ~~Meanwhile, we used the Particle Loss Calculator (PLC) to calculate the particle losses for the Model 3321 APS spectrometer in this cruise (Fig. 1) (Von Der Weiden et al., 2009). Fig, 1 showed that the particle losses were small in the size range from 0.5 μm and 10 μm.~~ Thereby, aerosol data within ~~the~~ size range of 0.5 to 10 μm were selected for ~~future~~ analysis in this study.

To further verify the accuracy of APS aerosol measurement results, we conducted a 15-day field inter-comparison experiment, using multiple aerosol instruments to validate the APS. A detailed description of this field inter-comparison experiment was provided in Supplement S1. By comparing aerosol size distributions measured by the three instruments (Fig. S2a), the good consistency confirms the accuracy of the APS in capturing aerosol particle distributions. Since direct channel-to-channel matching was not feasible due to the differing size bins for different aerosol measurement instruments, we compared total NCs within overlapping ranges: 0.5-1.981 μm for APS, 0.475-1.99 μm for Portable Optical Particle Spectrometer (POPS) (Handix Scientific, USA), and 0.488-2.14 μm for Model 11-D Portable Aerosol Spectrometer (GRIMM, Germany). All three instruments exhibited consistent diurnal trends (Fig. S2b). Fig. S3 showed high correlations between APS and the other instruments. The consistent trends and strong correlations further validate accuracy of the APS. Furthermore, during instrument channel matching, we observed that the APS lacks the standard 2 μm size bin typically used to distinguish accumulation mode and coarse mode particles. The closest available diameter in APS channels is 1.981 μm. A distinct peak consistently appeared at this size in aerosol size distributions. Based on these observations, we established 1.981 μm as the threshold for separating accumulation mode (0.5 μm ≤ Dp ≤ 1.981 μm) from coarse mode (1.981 μm < Dp < 10.37 μm) aerosols.

The ~~Model 3321~~ APS ~~spectrometer~~ was loaded in the captain's cabin and coupled with a 10-cm long tube and a 1.8 cm internal diameter, as shown in Fig. ~~2~~1a. The tube was fixed in an exterior wall of the captain's cabin at 30° to the horizontal and faced the direction of the sea surface. Meanwhile, the tube's inlet was approximately 7 m above the mean water level, and this location was thought to be less affected by human factors and ~~the~~ bow splashing. The flow rate was 1.0 liter per minute, and ~~the~~ sample length was 15 seconds. The atmospheric aerosol data resolution was set to 5 min in this SCS cruise observation. The detailed definition and calculation formula for aerosol number concentration were shown below.

$$N = \frac{C}{LQ} \times \frac{H}{K},$$

where ~~n~~N is the number concentration per channel, ~~e~~C is the particle counts per channel, L~~t~~ is the total sample time, Q is the sample flow rate, ~~Φ~~H is the sample dilution factor, and ~~η~~K is the sample efficiency factor per channel.

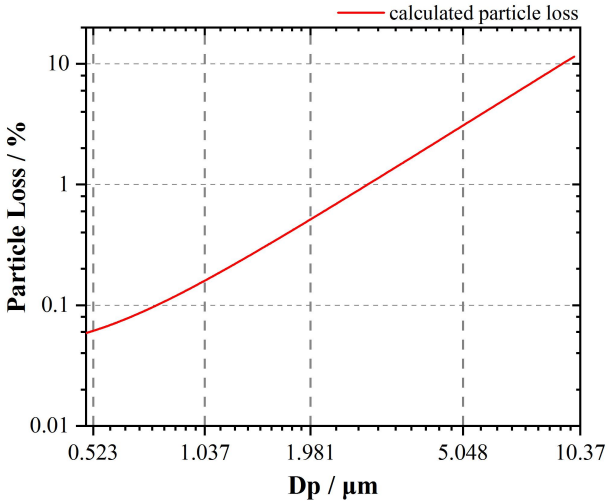

~~Fig. 1 The calculated particle losses for the Model 3321 APS spectrometer in this cruise.~~

2.2.2. Meteorological instruments

The automatic meteorological observation system (AMOS), including the Vaisala WXT530 weather station, the Campbell CSTA3B sonic anemometer, and the Belfort Model 6400 visibility sensor, was installed on the top deck to continuously ~~observe~~collect ~~the~~ meteorological ~~observation data~~observational data. The height of the AMOS above the mean water level was approximately 10 m, as shown in Fig. ~~2~~1b. The Vaisala WXT530 measured ~~the~~ atmospheric parameters such as air temperature (T_{OBS}), RH and rainfall intensity with a temporal resolution of 1 s. The two-dimensional wind field (i.e.~~,~~ ~~the~~ horizontal components u_x and u_y) was measured by the Campbell CSAT3B, with~~and~~ its ~~the~~ temporal resolution ~~was~~being 0.05 s. To support ~~the~~ ancillary research, the Belfort Model 6400 observed ~~the~~ atmospheric visibility (VIS) with a temporal resolution of 1 s. More detailed ~~descriptions~~sepcifications of the AMOS were provided~~listed~~ in Table 1.

Table 1

Configurations and specifications of AMOS

WXT530		CSTA3B		Model 6400	
Performance index	Description	Performance index	Description	Performance index	Description
Observation Range (T_{OBS})	-52 ~ +60 ℃	Observation Range (WS)	0 ~ 60 m s^{-1}	Observation Range (VIS)	0 ~ 50 km
Resolution (T_{OBS})	0.1 ℃	Resolution (WS)	0.1 m s^{-1}	Resolution (VIS)	0.1 km
Accuracy (T_{OBS})	±0.3 ℃	Accuracy (WS)	±0.3 m s^{-1}	Accuracy (VIS)	±1 km
Observation Range (RH)	0 ~ 100 %	Observation Range (WD)	0 ~ 360°		
Resolution (RH)	0.1 %	Resolution (WD)	1°		

Accuracy (RH)	±3 %	Accuracy (WD)	±3°
Observation Range (Rain)	0 ~ 200 mm h^{-1}		
Resolution (Rain)	0.1 mm h^{-1}		
Accuracy (Rain)	±0.5 mm h^{-1}		

Fig. ~~2~~1 The total view of (a) the Model 3321 APS spectrometer and (b) the automatic meteorological observation system.

2.3. Auxiliary data

2.3.1. Reanalysis data

In this study, ~~the~~ 10-m wind speed (WS_{10}), direction (WD_{10}), and friction velocity (U_{zust}) were obtained from the ERA5 hourly dataset with a spatial resolution of 0.25° × 0.25°. The ERA5 hourly dataset used in this study was provided by the

European Centre for Medium-Range Weather Forecasts (ECMWF) (Hersbach et al., 2023). In order to determine ~~the~~ values of SST-T_{2m}, we needed to know ~~the~~ temperature at 2 m (T_{2m}) and SST. ~~Meanwhile, t~~The Modern-Era Retrospective Analysis for Research and Applications,~~Merra-2~~ Version 2 (MERRA-2) published SST and T_{2m} reanalyzed data were~~as~~ in excellent agreement with the observational data~~observed SST data~~ in the SCS ($r > 0.9$) (Jiang et al., 2021). We selected ~~the~~ SST and T_{2m} data from the MERRA~~erra~~-2 meteorological dataset in this context (Gelaro et al., 2017).

For ~~the~~ atmospheric aerosol component data, the NASA Goddard Space Flight Center MERRA~~erra~~-2 aerosol dataset was used in this study due to its good performance over Europe and China (Provençal et al., 2017a, ~~&~~ 2017b). The MERRA~~erra~~-2 aerosol dataset ~~consisted of~~includes the assimilated aerosol diagnostics data, such as ~~the~~ surface mass concentrations of aerosol components (~~i.e.~~e.g. , ~~sea~~ salt ($SEAS_{10}$; $Dp \leq 10$ μm), dust ($DUST_{10}$; $Dp \leq 10$ μm), black carbon (BC), sulfate (SO_4^{2-}), and organic carbon (OC)) with a spatial resolution of 0.5° × 0.625° and a temporal resolution of 1 hour (Randles et al., 2017~~Global Modeling and Assimilation Office (GMAO), 2015~~). We used ~~the~~ above aerosol component data to discuss ~~the~~ discrepanc~~ies~~y in aerosol distribution over the SCS.

2.3.2. Back trajectory analysis

The Hybrid Single-Particle Lagrangian Integrated Trajectory (HYSPLIT) transport and dispersion model (http://www.arl.noaa.gov/ready/hysplit4.html), developed by the National Oceanic and Atmospheric Administration Air Resources Laboratory (NOAA ARL), was employed to analyze ~~the~~ air mass backward trajector~~ies~~y. The meteorological data for the backward trajectories were~~as~~ obtained from the Global Data Assimilation System (GDAS) archive dataset (http://ready.arl.noaa.gov/gdasl.php). The backward trajectories were calculated for 72 h. ~~Meanwhile, t~~The trajectories were calculated at an altitude of 50 m, and the top of the HYSPLIT model was set to 5,000 m to clarify the influence of the source region on the marine aerosols.

2.3.3. Distances from the coast

The ArcGIS path distance method was used to calculate distances from the coast. In equidistant projection, ship positions were used as input data, and coastline position data were used as reference lines for distance analyses. Considering the actual surface distance as well as horizontal and vertical factors, the shortest distance from the ship to the coastline can be calculated.

2.4. Contaminated data screening

To observe actual aerosol loadings in the typical marine environment, it is necessary to exclud~~cing~~ aerosol ~~observation data~~observational data contaminated by ship emissions during the cruise (including ~~the periods subject to the offshore and the pelagic~~data collected in offshore and pelagic regions)~~ is necessary~~. To achieve this, we performed quality control during

~~the~~ aerosol ~~observation data~~observational data collection with ~~the~~ accompanied WS, WD, rainfall intensity, and ~~total aerosol number concentration~~NC observational data as follows:

i) *Data screening with wind observations*. The north arrow of the Vaisala WXT530 was oriented perpendicular to the ship's longitudinal axis, pointing east relative to the vessel's heading. ~~The o~~Observed WD thus represented the relative angle between the wind direction and the ship's course. When the ~~the~~ ship was sailing, ~~the~~ WD sampled ranged from 225° to 315°. We excluded these ~~sampled~~ data because ~~the~~ aerosol observations were directly affected by the ship emissions. As depicted in Fig. ~~3~~2a, ~~one can easily find~~ a sharp decrease and subsequent increase in the observed aerosol size distributions can be easily identified on 25 May. The underlying cause of ~~the~~ abnormal changes in aerosol size distribution could be the removal of ~~the~~ coarse aerosol mode by ~~the~~ rainfall, as depicted in Fig. ~~3~~2b. However, this "jump" was located at 7:00 a.m. (circled in black in Fig. ~~3~~2a) while the rainfall occurred at 8:00 a.m. and lasted for ~~about~~approximately 6 hours, so it is not the rainfall that influences the data jump in aerosol size distribution. With the help of ~~the~~ WD sequence data shown in Fig. ~~3~~2b (circled in red), we found that the jump in ~~the~~ WD curve was also located at 7:20 a.m. and thus identified the accurate cause of ~~the~~ aerosol data jump; it was~~is~~ ~~the~~ wind direction rather than ~~the~~ rainfall that led to the anomaly in aerosol size distributions.

ii) ~~ii)~~ *Further data screening with unreasonable NCs*. ~~The new aerosol generation events often accompanied the increased nucleation events.~~ Aerosol NCs remain relatively constant under stable meteorological conditions (Hoppel, 1979, 1985; Russell et al., 1996). In the presence of continental transport, sustained high NCs would persist for several hours (Saha et al., 2022; Wang et al., 2020). Therefore, ~~The previous studies indicated that the nucleation events observed in marine environments were characterized by different shapes, in the aerosol size distributions versus time series plots. However, all the nucleation events last at least several hours at the sea surface (Kuang et al., 2009; Ehn et al., 2010), due to the persistent growth of these aerosol particles. So, w~~we ~~excluded the sharp decrease and increase in NCs data in the short term without changes in ~~the~~ meteorological parameters and influences of continental transport, and all ~~the~~ excluded data had NCs that were one order of magnitude higher or lower than the average NC at that time. ~~So~~So as to ~~that~~ further screen out the possible influences produced by the ship emissions.

Applying these criteria, 88 % of the observational data in this cruise were retained for analysis.

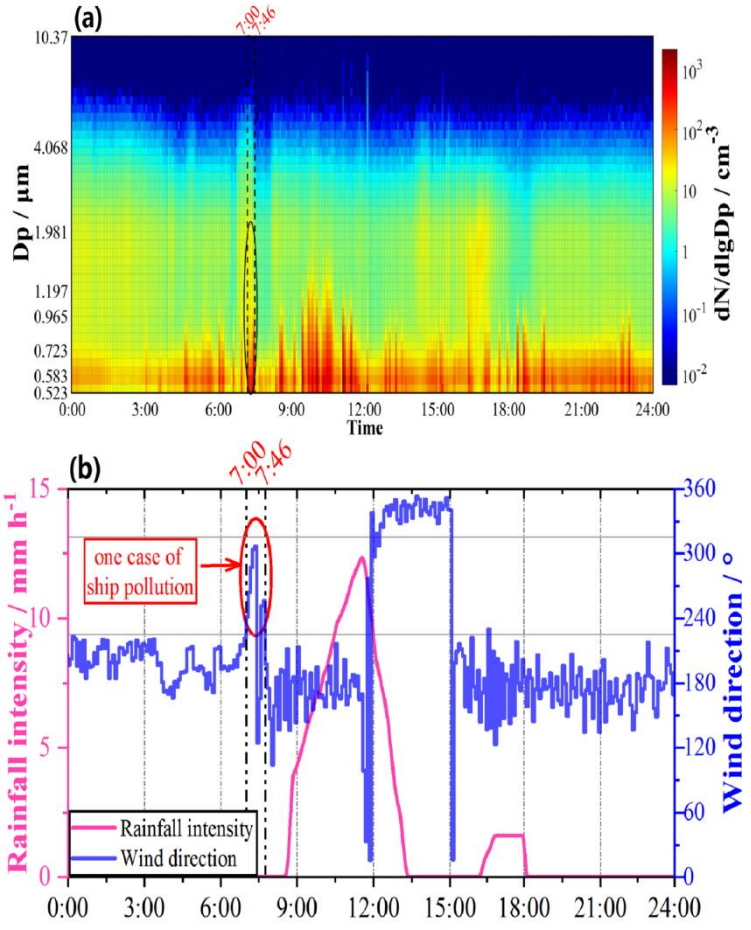

270 **Fig. ~~3~~2 The time series of the observations on 25 May 2023. The black circle represented one case of ship pollution. (a) Trends of the aerosol size distributions. (b) Trends of the rainfall intensity and the WD.**

3. Results and discussion

3.1. Temporal distributions of the observations

Fig. 4~~3~~ showed the time series of ~~the~~ marine aerosol distributions and ~~the~~ meteorological parameters during the observation 275 ~~of the~~ shipboard in the SCS. Due to the pump of the Model 3321 APS spectrometer failing to work from 4 June to 15 June 2023 during the cruise period, ~~the~~ flow rate could not reach the minimum standard. Thus, we only analyzed variations of ~~the observation data~~observational data from 21 May to 3 June 2023. Fig. 4~~3~~ a-b presented the trends of ~~the~~ aerosol size distribution and ~~the~~ comparison of the accumulation (0.5 μm ≤ Dp ≤ 1.981 μm) and coarse (1.981 μm < Dp < 10.37 μm) mode particle NCs. During the shipboard observation period, the average ~~total marine aerosol~~summed (Dp < 10.37 μm) NC 280 was 54.01 ~~± 35.37~~ cm^{-3}, ~~the~~ NC of aerosol accumulation mode was 52.35 ~~± 34.96~~ cm^{-3}, and ~~the~~ NC of aerosol coarse mode

was 1.66 ~~± 0.83~~ cm^{-3}. For these three aerosol modes, the NCs varied from 18.46 to 89.38 cm^{-3}, 17.39 to 87.31 cm^{-3}, and 0.83 to 2.49 cm^{-3}, respectively, during the shipboard observation period, exhibiting substantial temporal fluctuations.~~We found that the marine aerosol NC changed drastically with the temporal differences during the shipboard observation period. Meanwhile, the p~~Published ~~observation data~~observational data of ~~the~~ marine aerosol NC relevant to this study were shown in Table 2. ~~Due to the constraints of the geographical location and the data acquisition, we listed some relevant shipboard observation data.~~ The shipboard observational data showed overall average values and standard deviations of maritime aerosol NCs under different temporal and geographical conditions. We used these data to compare with the marine aerosol NCs during this cruise period. ~~The shipboard observation data recorded and showed the overall average values and standard deviations of marine aerosol NCs under different temporal and geographical conditions, which were used to compare with the marine aerosol NCs observed.~~

In this study, ~~the~~ observed NC of accumulation mode was ~~more consistent with the 2005 SCS observation (Lin et al., 2007) but~~ lower than the observation in the East China Sea (Lin et al., 2007; Ma et al., 2022). Aerosol emissions from the Yangtze River Delta region are higher than those from the Pearl River Delta region (Li et al., 2017). Due to the influence of aerosol transport, a greater amount of continental and anthropogenic aerosols from the Yangtze River Delta were delivered to the East China Sea compared to the amount transported from the Pearl River Delta to the South China Sea.~~This suggested that the NC of aerosol accumulation mode in the East China Sea might affected by the higher frequency of the new marine aerosol particle formation and the more frequent continental source transport at the westerlies.~~ Hence, the ~~aerosol~~ accumulation mode NC was significantly lower in the SCS. The SCS is one of the marginal seas of the Western Pacific~~Meanwhile,~~, T~~t~~he ~~total marine aerosol~~total NC observed in this study (54 cm^{-3}) ~~contained the aerosol coarse mode (2 μm ≤ Dp ≤ 10 μm) and the part of aerosol accumulation mode (500 nm ≤ Dp ≤ 2000 nm), and the NC~~ was slightly lower than ~~the marine aerosol~~ NC in the Western Pacific (83 cm^{-3})~~Atlantic~~ by Flores et al. (2020). Regarding the marine aerosol NCs in the same ~~region~~ocean area, the observations of Cai et al. (2020) and Kong et al. (2016) were significantly higher than the observations in this study. Although the differences in the observation seasons~~, the study region,~~ and the particle size might influence~~d~~ the average NC observations, these differences may still indicate that~~it can still show that~~ the marine aerosol was significantly affected by the continental transport and the anthropogenic activity in the offshore ~~area~~regions, based on~~according to~~ the latitude and longitude.

Wet deposition through scavenging by rainfall ~~process~~ is a critical sink for aerosols (Atlas & Giam, 1998; Radke et al., 1980). ~~.~~ However, intense precipitation events might paradoxically elevate aerosol Ns.~~However,~~ Ssome studies indicate that impaction of liquid droplets on porous surfaces (e.g. the ship surfaces) may generate aerosol particles~~found that the aerosols might be generated on the porous surface when impinged by liquid droplets~~ (Bird et al., 2010; Joung & Buie, 2015; Zhou et al., 2020). ~~Thereby~~By accounting for ~~the~~ observation environment and rainfall intensity, short-duration heavy rainfall resulted in numerous raindrops impacting the ocean and ship surfaces, generating aerosol particles. Subsequently, the monitoring instrument captured some of these aerosol particles, ultimately contributing to the increased aerosol particle concentration observed in Fig. 43 (the blue-shaded regions). In addition to the elevated concentrations of marine aerosols

resulting from these rain events, the aerosol NC spectrum distributions shown in Fig. 43a demonstrate continuous marine aerosol number concentration distributions in the size ranges of 523 to 583 nm, 1715 to 1981 nm, and 3786 to 40684371 nm during the cruise period.; whichThis indicated the background characteristics of marine aerosol particle distributions in the marine environment. Meanwhile, dDuring the cruise period, comparisons of the time series of the NCs between the two aerosol particle modes were made, as shown in Fig. 43b. The temporal trend of the NC of accumulation mode was approximately consistent with the coarse mode. The correlation coefficient between the these twowo aerosol particle modes was approximately R = 0.71. However, there were some discrepancies in the NC of the different particle sizes in aerosols caused by the different marine aerosol sources.; Wand we also found that the temporal trend of the accumulation mode was more variable than that ofe coarse mode.. Therefore,suggesting the accumulation mode waswas may be more obviously influenced by changes in the marine environment.

For the meteorological parameters, the ship remained in the northeast trade winds during the wholeentire cruise period; therefore, this mainly led to the sSouth-wWesterly and sSoutherly winds, as shown in Fig. 43c. Fig. 43d represented the air temperature and the water temperature. The observed air temperature was in excellent agreementconsistent with MERRA-2 the reanalyzed air temperature from Merra-2(R = 0.719), whereas the average T_{2m} and SST over the whole observation period were closer to 29.0 ℃ and 29.7 ℃, respectively. The RH had an obvious negative correlation with the visibility (R = -0.74), and the average RH and VIS were equal to 83.0 % and 45.1 km. Meanwhile, due toSince wind is abeing the major driver of marine aerosol the production and transport of marine aerosols, we attempted to explain marine aerosol NCs of the accumulation mode and the coarse mode as the functions of the WS and WD (Fig. 54a, b). The RH and the rainfall intensity observations were used to aid analysis (Fig. 54c, d). High NCs (≥ 150 cm^{-3}) were observed almost entirely in which the WD were between NW and N that were caused by the high RH accompanied by the rainfall events, and the distributions of NCs were uniform when the wind was blowing in the other directions.

Fig. 65 showed the variations of the NCs of two aerosol particle modes with the WS, and the observation dataobservational data were binned to theat 3 m s^{-1} WS intervals equal to 3 m s^{-1}. The variations in the NCs with the WS observed in this study were in accordanceconsistent with thea previous study (Bruch et al., 2023). For example, marine aerosol NCs generated by the bubble bursting process at low WS showed little variation, and the low WS was insufficient to activate spume droplet production. Consequently, no significant variation in NCs were observed in the 0-6 m s^{-1} WS range.For example, the NCs changed little in the region of 0-6 m s^{-1} WS because the WS was low for activation of the spume droplets and the marine aerosol generations. The NCs obviously increased with the increase in WS from 6 m s^{-1} to 15 m s^{-1}; however, the increase slowed down when the WS exceeded 13 m s^{-1}. TheThe previous study proposed that thise phenomenon may wasbe linked to the scavenging of marine aerosols through aerosol collision by the larger water drops at high WS (Pant et al., 2009).

Table 2

Summary of the available study results on the shipboard observation of ved marine aerosol NC (cm^{-3})

Region	Time	Latitude Season	Latitude Longitu	Longitude Parameter	Parameter Value	Value Param eter	Parameter Value	Value Refe rence	Reference
South China Sea	2023.05 - 2023.06	21°N – 8°N Spri	21°N - 8°N 115	115°E - 110°E Aec	Accumulation mode (n500-	52.4 ± 35.0 n500-10000	n500-10000 54.0 ±	54.0 ± 35.3 This	This Study
South China Sea	2018.08	23°N – 19°N	23°N - 19°N 11	118°E - 108°E n10-	n400-32000 3400	61 n400-32000	61	Cai et al., 2020	Cai et al., 2020
South China Sea	2012.09 - 2012.10	21°N – 20°N	21°N - 20°N 11	118°E - 113°E n120	n120-10000 175	175		Kong et al., 2016	Kong et al., 2016
South China Sea	2005.05	20°N – 18°N	20°N - 18°N 11	118°E - 113°E Aec	Accumulation mode (n50-	50.3 ± 19.5		Lin et al., 2007	Lin et al., 2007
East China Sea	2005.05	Spring 3 0°N –	30°N - 26°N 12	122°E - 117°E Aec	Accumulation mode (n50-	109.2 ± 51.8		Lin et al., 2007	Lin et al., 2007
East China Sea	2017.04 - 2017.05 20	28°N – 20°N	28°N - 20°N 13	130°E - 120°E n250	n250-2500 57.4 ± 40.9	57.4 ± 40.9 n2500-	n2500-10000 57.5 ±	57.5 ± 41.3 Ma et	Ma et al., 2022
Western Pacific Atlantic	2017.04 - 2017.05 6	Spring 6 0°N –	20°N - 0°N 80°	180°E - 130°E n100	n100-19800 83	83 ± 30		Flores et al., 2020	Flores et al., 2020
North Atlantic	2015	50°N	4°W	n1000-6000	24			Yang et al., 2019	

Note. In the column of the "Parameter", "n" indicated the NC and the subscripts indicated the particle size (nm); in the column of the "Latitude", "N" represented north latitude. The results of this study and these references were the overall average aerosol NCs.

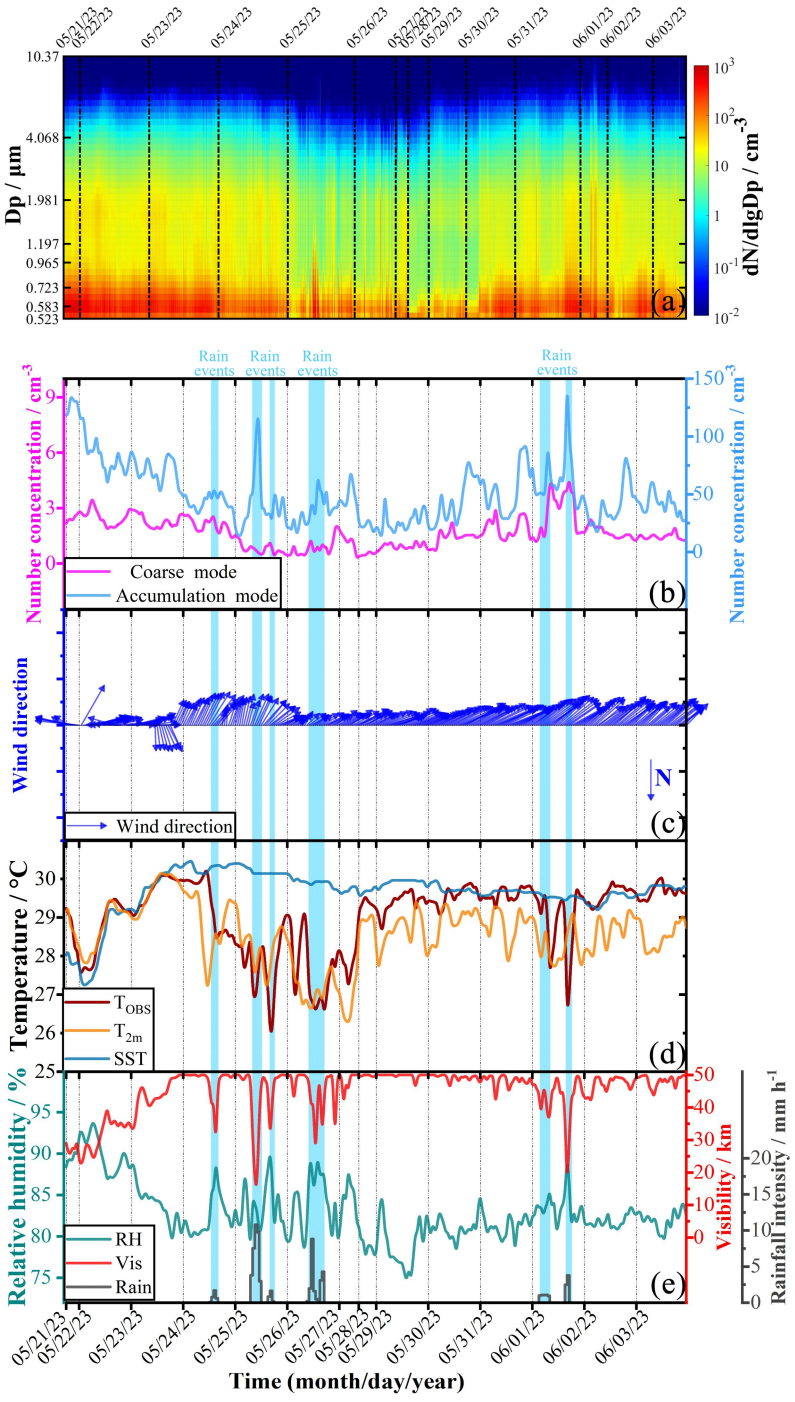
Dp / μm
dN/dlgDp / cm-3
(a)
Rain events
Number concentration / cm-3
Coarse mode
Accumulation mode
(b)
Wind direction
N
Wind direction
(c)
Temperature / °C
TOBS
T2m
SST
(d)
Relative humidity / %
Visibility / km
Rainfall intensity / mm h-1
RH
Vis
Rain
(e)
Time (month/day/year)

350

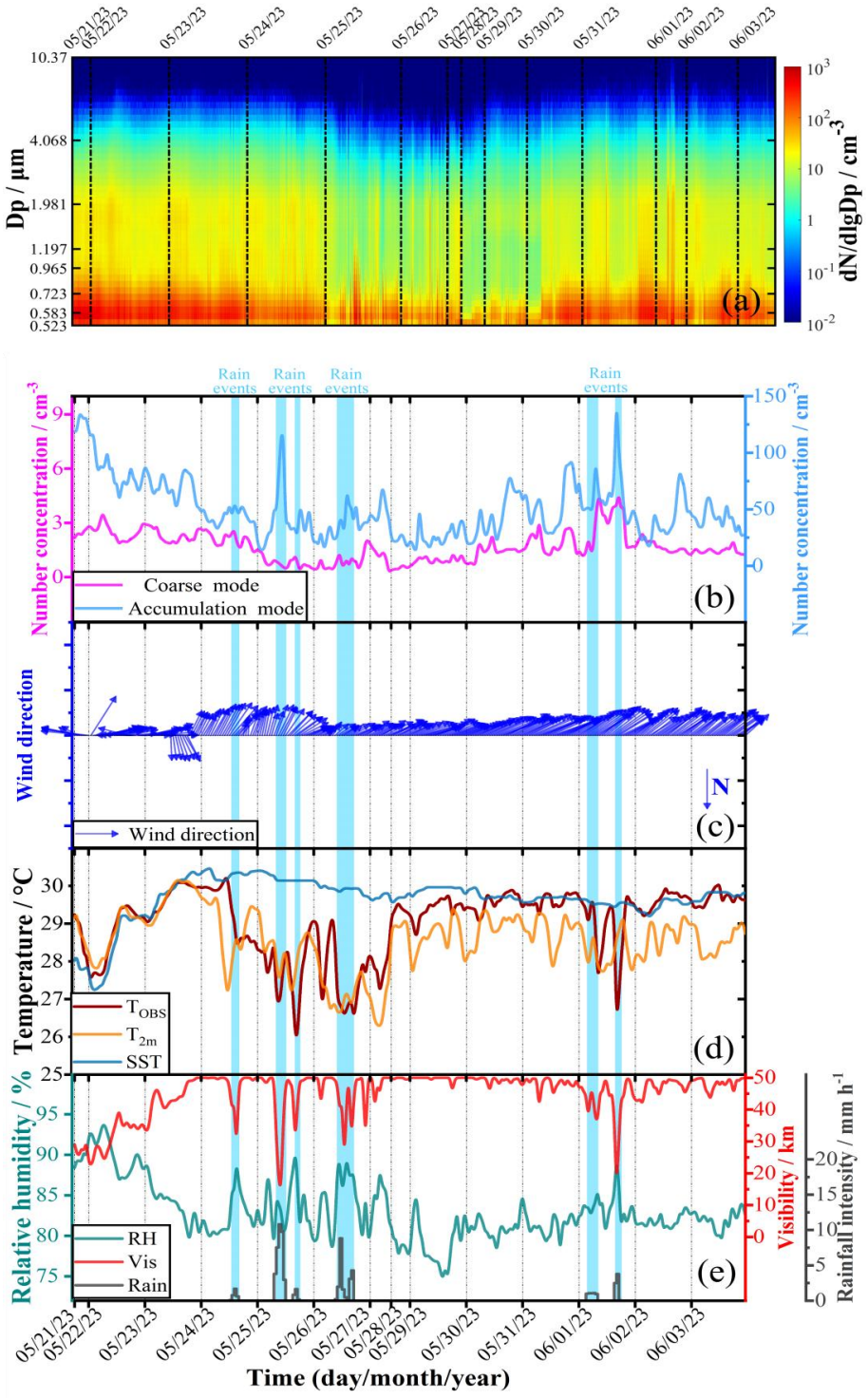
Dp / µm
dN/dlgDp / cm-3
(a)
Rain events
Number concentration / cm-3
Coarse mode
Accumulation mode
(b)
Wind direction
N
(c)
Temperature / °C
TOBS
T2m
SST
(d)
Relative humidity / %
Visibility / km
Rainfall intensity / mm h-1
RH
Vis
Rain
(e)
Time (day/month/year)

Fig. 43 The time series of the shipboard observations in the SCS from 21 May to 3 June 2023. The blue-shaded regions represented periods affected by rain events. (a) Trend of the aerosol size distributions. (b) Trends of NCs of the two aerosol particle modes (black solid line represented the NC of the coarse mode, and red solid line represented the NC of the accumulation mode). (c) Trend of the WD. (d) Trends of the T_{OBS} (dark orange solid line), T_{2m} (light orange solid line), and SST (blue solid line). (e) Trends in the RH (gray solid line), the VIS (red solid line), and the rainfall intensity (dark blue solid line).

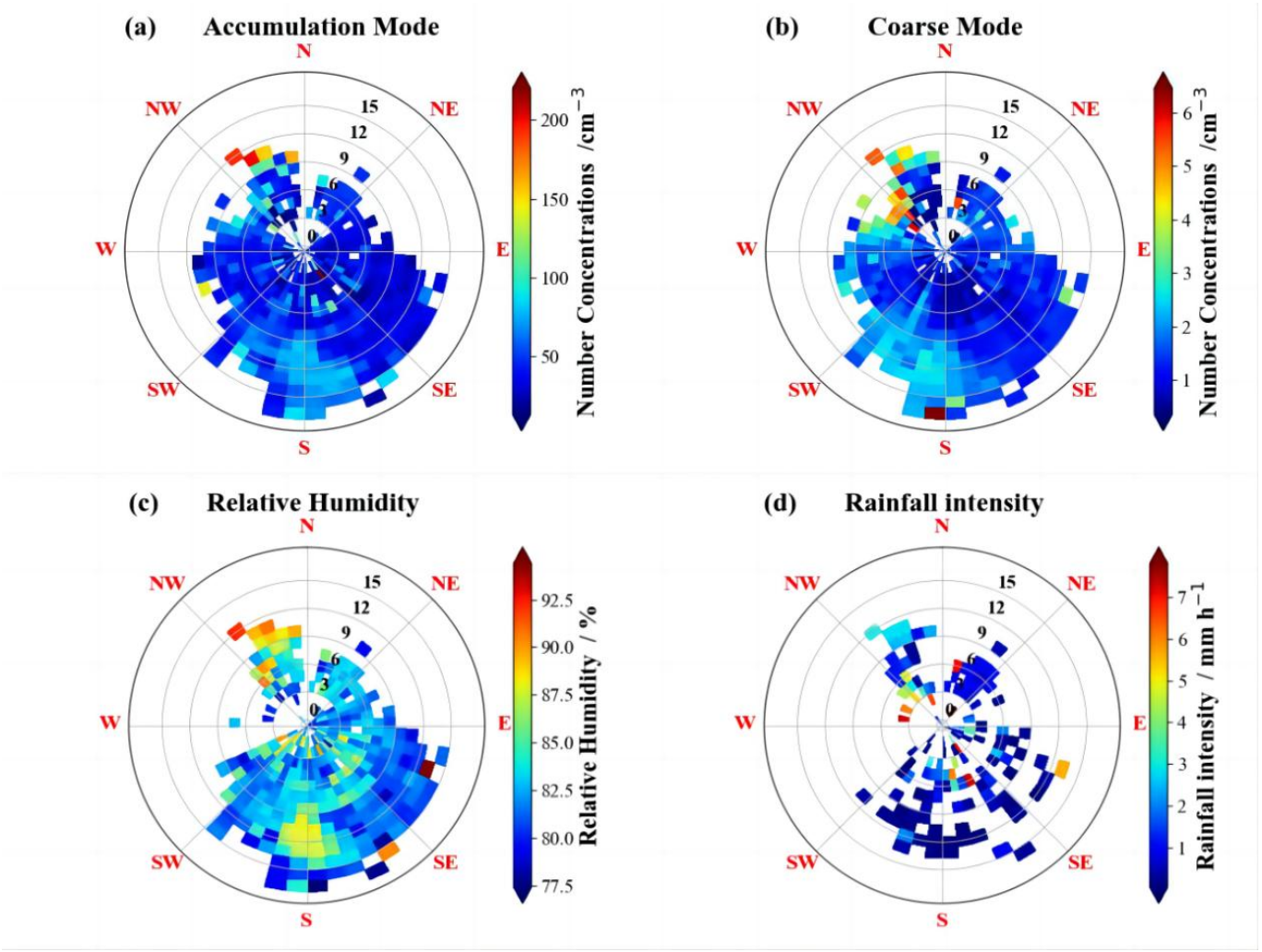

Fig. 54 (a) NC of the aerosol accumulation mode, (b) NC of the aerosol coarse mode, (c) RH, and (d) rainfall intensity as the functions of the WS and WD for the observations in the SCS.

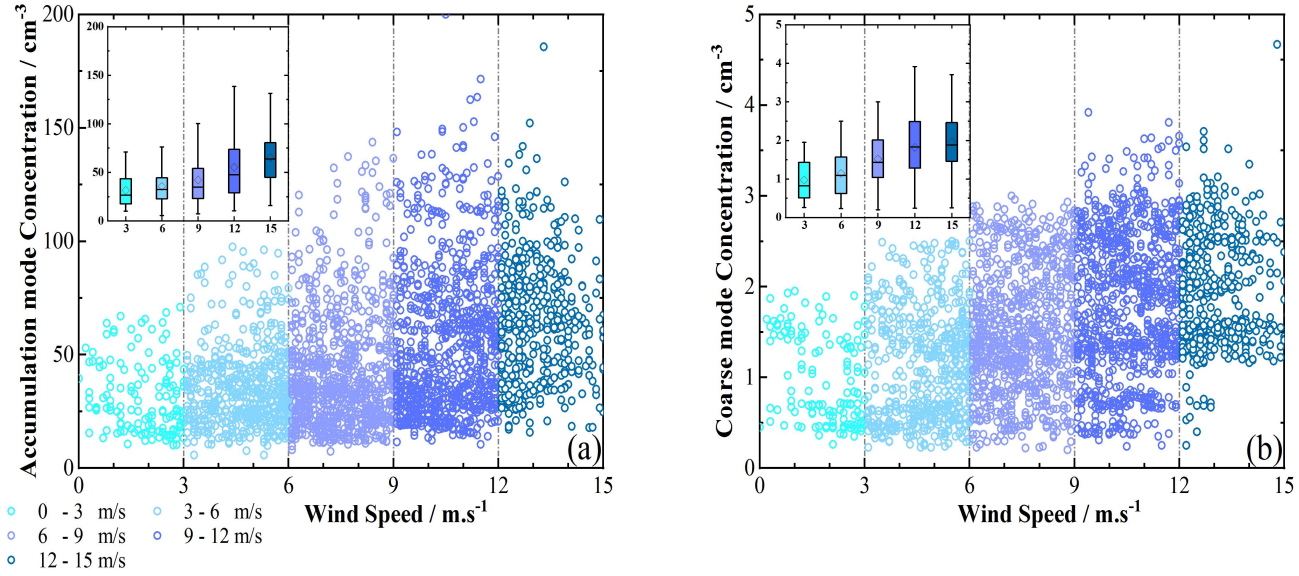

Fig. ~~6~~5 The scatter plots of (a) NCs of the aerosol accumulation mode and WS, (b) NCs of the aerosol coarse mode and WS. The ~~observation data~~observational data were binned to the WS intervals equal to 3 m s^{-1}; the boxes represented the 25th to 75th percentile value, the black whisker represented the 1.5 inter-quartile range, the black diamond marker represented the mean value, and the black horizontal line represented the median value in the box plots.

3.2. Marine aerosol distributions in the different distance from the coast

This marine scientific research campaign started southward from the harbor of Zhanjiang (21°16′21.12″ N, 110°23′45.17″ E) on 21 May and reached up to the southernmost (8°5′ N) point of this cruise on 3 June. In ~~the~~ different latitudes of the SCS, there were vastly different marine aerosol distribution characteristics, meteorological parameters, and marine aerosol transport sources. Therefore, we assessed ~~the~~ features of ~~the~~ marine aerosol distribution at various ~~distances from the coast~~distances from coast. ~~We used the ArcGIS path distance method to calculate the distances from the coast and analyze the influences of distances on marine aerosols. In the equidistant projection, the ship positions were used as the input data, and the data of the coastline positions were used as the reference lines for the distance analyses. Considering the actual surface distance and horizontal and vertical factors, the shortest distance can be calculated from the ship to the coastline positions.~~ We conducted real-time analysis of the 72-hour backward trajectories of air masses at the ship's location (Fig. 6a, b). The backward trajectory analysis indicated that the air masses had last passed over continental areas on 22 May 2023, 11:00 local time (LT), at a point 50 km from the coast (the red solid lines in Fig. 6b). Consequently, for all sampling locations within this 50 km boundary, the air masses had directly passed over mainland areas. This meant they carried continental and anthropogenic aerosols that ultimately influenced the aerosol distributions (Braun et al., 2020; Wu & Boor, 2021). For regions more than 50 km from the coast, the backward trajectory results consistently showed that the air masses did not pass over any mainland areas before reaching the sampling site (the blue solid lines in Fig. 6a). The prevailing wind direction was primarily from the southwest (Fig. 3c) in these regions, so aerosols could not be directly transported from the

continent to the ship's location. Additionally, continental and anthropogenic aerosols, which were emitted from islands and countries surrounding the SCS, lost their original characteristics through the long-duration (over 72 hours) transport. These aerosols underwent atmospheric long-range transport, dry deposition, wet deposition, and aging processes. Such processes led to the removal of continental aerosols or their gradual dilution and mixing with natural aerosols (Hodshire et al., 2019;Ohata et al., 2016; Xu et al., 2021). Over time, the continental and anthropogenic aerosols transformed or integrated into the background aerosols. Hence, 50 km from the coast was taken as the boundary distance to distinguish offshore and pelagic regions in this study. ~~Meanwhile, the distance from the coast of 50 km was taken as the boundary distance to distinguish the offshore and pelagic regions in this study. Hence, w~~We ~~could~~can analyze ~~the~~ differences in aerosol transport and ~~generation~~production in ~~the~~ offshore and pelagic regions. To eliminate the effects of rainfall on aerosol concentrations, ~~Meanwhile, w~~we removed ~~the~~ aerosol data~~, which was~~ associated with rainfall intensity greater than 1 mm h^{-1} ~~rainfall intensity~~ during~~in~~ the observation ~~time~~period.~~, to eliminate the effects of the wet deposition on aerosol generation.~~

Fig. 7 ~~showed~~revealed ~~the~~ marine aerosol distribution characteristics with different modes in the SCS. From Fig. 7a, we can find that ~~the~~ NCs of different aerosol particle modes in ~~the~~ offshore ~~area~~regions showed significant differences from those in ~~the~~ pelagic ~~area~~regions. The average total NC ~~of the total marine aerosols~~ in ~~the~~ offshore ~~area~~regions during the cruise period was 108.25 cm^{-3}, registering a ~~1~~2.2-fold increase compared to~~times higher than the~~ NC in ~~the~~ pelagic ~~area~~regions (49.22 cm^{-3}). ~~Meanwhile, t~~The NC of ~~the~~ accumulation mode in ~~the~~ offshore ~~area~~regions was 105.57 cm^{-3}, and it was 47.65 cm^{-3} in ~~the~~ pelagic ~~area~~regions. The average ~~NC of the~~ accumulation ~~aerosol~~ mode NC in ~~the~~ offshore ~~area~~regions was ~~1~~2.2 times higher than that in ~~the~~ pelagic ~~area~~regions, with a statistically difference ($p < 0.001$). Similarly, the comparison of the coarse mode NC revealed the same result as that for the accumulation mode. The coarse mode NC in the offshore regions (2.68 cm^{-3}) was also significantly higher than that in pelagic regions (1.57 cm^{-3}), with a statistically significant difference ($p < 0.001$).~~However, the NC of the coarse mode comparison revealed that the result differed from the accumulation mode comparison, with little differences in the offshore and pelagic regions, where the NCs of the coarse mode in the offshore areas were 2.68 cm^{-3} and 1.57 cm^{-3} in the pelagic areas.~~ Fig. 7b showed the number size distribution for marine aerosols of 0.5 to 10 μm diameters in the offshore and pelagic regions, where ~~the~~ $dN/dlgD_p$ represents the number size distribution. The comparisons in Fig. 7b showed that the number size distributions in the offshore and pelagic regions ~~showed~~exhibited ~~the~~ a bimodal distribution, and the peak values both occurred at 0.542 and 1.981 μm, which were consistent with the previous studies (Andronache, 2003; Braun et al., 2020)~~ marine aerosol particle sizes~~. The number size distributions exhibited a relatively stable value in the 0.835-1.981 μm particle size range. Due to aerosol transport, continental air masses may have carried continental and anthropogenic aerosols, which could have ultimately affected aerosol distributions in the 0.5-5.0 μm particle size range. The number size distributions in the offshore regions were obviously higher than in those the pelagic regions in the 0.5-5.0 μm particle size range. These findings were consistent with previous studies (Braun et al., 2020; Lorenzo et al., 2023). However, in the 5.0-10 μm particle size range, the number size distributions from offshore and pelagic areas exhibited close agreement, demonstrating consistent correlation patterns that remained robust against instrumentation limitations. This comparability persists despite APS measurements in this range having inherent uncertainties reaching up to

130% (Pfeifer et al., 2016), primarily due to inefficient particle detection at concentrations approaching 1 cm^{-3}. Throughout the cruise, continuous 5-second sampling yielded 64,180 valid samples, which through statistical averaging reduced measurement uncertainty to 0.5%. At this negligible level, the distribution characteristics and cross-regional correlations are considered reliably preserved. ~~However, in the 5.0-10 μm particle size range, the number size distributions in the offshore areas were in excellent agreement with those in the pelagic areas~~.

~~It was obvious from~~ Fig. 7c revealed ~~that~~ a decreasing trend in NCs with increasing distance from the coast~~the NC was highly correlated with the distance from the coast,~~, ~~and~~ the correlation coefficients between the daily average NCs of accumulation mode, coarse mode, and the total NCs and the distance from the coast were calculated as R = -0.87, -0.67, and -0.81, respectively. The correlation analysis, based on hourly average NCs of accumulation and coarse modes versus the distance from the coast, yielded R = -0.59 and -0.50 for offshore regions, and R = -0.28 and -0.33 for pelagic regions. The same was true for the total NC; the correlation coefficient between the hourly average total NC and the distance was -0.56 in the offshore regions and -0.29 in the pelagic regions. These correlations indicated that ~~the NC of the accumulation mode showed a significantly decreasing trend with the increasing distance from the coast (R = -0.87). We can find that R = -0.59 for the offshore distribution and R = -0.28 for the pelagic distribution, which showed that~~ the correlation between distance from the coast and NC ~~of accumulation mode~~ was mainly reflected in the offshore ~~area~~regions and had almost no ~~influence~~ significant correlation ~~on~~with ~~the~~ marine aerosol in the pelagic ~~area~~regions. ~~The same was true for the coarse mode; the correlation between the coarse mode and the distance was -0.50 in the offshore areas and -0.33 in the pelagic areas.~~ In offshore regions, aerosol NC was influenced by continental aerosol transport. This influence diminished with increasing distance from the coast.~~In other words, the aerosol distribution in the near-land and offshore regions was accompanied by the obvious aerosol transport phenomenon.~~ After the ship entered the pelagic ~~area~~regions, the influence of continental air mass transport~~air mass transport~~ almost disappeared. M~~The m~~arine aerosol NCs were lower in pelagic regions compared to offshore regions.~~had been kept lower in the pelagicarea.~~

~~From~~ Table 3 revealed discrepancies in meteorological parameters between offshore regions and pelagic regions. ~~, we can see that the meteorological element distributions in the offshore areas were significantly different from those in the pelagic areas.~~ For example, the average WS in ~~the~~ offshore ~~area~~regions was 10.74 m s^{-1}, slightly higher than that in ~~the~~ pelagic ~~area~~regions (8.64 m s^{-1}). Higher WS can enhance marine aerosol production. Therefore, there ~~was~~was a higher ~~generation~~production of aerosols in ~~the~~ offshore ~~area~~regions. In addition ~~to the WS influence~~, the offshore regions were relatively close to the coastline (Fig. 6b). Compared to pelagic regions, southwest and west winds in offshore regions could directly transport continental and anthropogenic aerosols to the ship's location from Guangdong and Hainan, China. Therefore, aerosol transport was higher in offshore regions.~~the frequency of southwest and west winds was high in the offshore environments. The distance from the coast ocean was short in the offshore region, which was accompanied by the aerosol transporting from Guangzhou and Hainan provinces, China (Fig. 8b).~~ ~~Fig. 8a showed the distributions of the backward trajectory air mass in the offshore and pelagic regions. The air masses passed over the mainland areas, which carried the continental aerosols and ultimately influenced the aerosol distributions in the offshore environments. However,~~

~~on the one hand, the prevailing wind direction was primarily from the southwest (Fig. 3c) during the pelagic observation period, and the air masses did not directly pass over the mainland areas. On the other hand, the continental and anthropogenic aerosols, which were emitted from islands and countries surrounding the SCS, underwent atmospheric transport, transformation, and deposition processes. This results in gradual dilution and mixing with natural aerosols. Over time, the continental and anthropogenic aerosols transformed or integrated into the background aerosol, losing their original characteristics (Gathman, 1983; Nascimento et al., 2021; Solomon et al., 2011). Therefore, in the pelagic environments, the marine aerosol was not significantly affected by aerosol transport and anthropogenic activity. There~~Fig. 7d ~~existe~~indicated~~d~~ a ~~significant~~ difference in the distribution~~s~~ of marine aerosol components between ~~the~~ offshore and pelagic regions ~~(Fig. 7d)~~. In the offshore regions, t~~T~~he proportions of ~~the~~ dust ($DUST_{10}$; Dp ≤ 10 μm) and sulfate aerosols (SO_4^{2-}) ~~in the offshore areas~~ were 5.04 % and 1.36 %, which were higher than those in the pelagic regions (1.45 % and 0.97 %, respectively)~~were~~. The higher concentrations of dust and sulfate aerosols may further ~~higher than those in the pelagic areas,~~ indicat~~e~~ing that ~~the~~ continental aerosol~~s~~ have ~~significantly~~ influenced the aerosol components in the ~~the~~ offshore ~~environment~~region~~s~~ (Geng et al., 2023; VanCuren, 2003). ~~. Meanwhile,~~In the pelagic regions, ~~due to the higher frequency of marine biological activities in the pelagic environments,~~ the proportions of ~~the~~ dimethyl sulfide (DMS), organic carbon (OC), and sulfur dioxide (SO_2) ~~aerosols~~ were 0.15 %, 1.2 %, and 1.7 %. These proportions were higher than those in the offshore regions (0.1 %, 0.84 %, and 0.56 %, respectively) due to the more frequent marine biological activities (e.g. phytoplankton metabolism) in the pelagic environments. For instance, phytoplankton releases DMS through cellular metabolism and lysis (Saliba et al., 2020); DMS then undergoes atmospheric oxidation to form SO_2 (Kettle & Andreae, 2000). Additionally, phytoplankton also produces OC (O'Dowd et al., 2004). These marine biological activities directly contribute to higher proportions of DMS, SO_2, and OC in pelagic regions. ~~and higher than those in the offshore environments, which were 0.1 %, 0.84 %, and 0.56 %, respectively.~~ The proportion of sea salt aerosol ($SEAS_{10}$; Dp ≤ 10 μm) in the pelagic ~~area~~region~~s~~ (94.33 %) was higher than that in the offshore ~~area~~region~~s~~ (~~94.33 % and~~ 91.9 %), reflecting higher marine aerosol production in the pelagic environments. To sum up, our results indicated that the distance from the coast had a great influence on marine aerosol production~~generation~~ and transport. It ultimately led to the obvious discrepancy between ~~the~~ size distributions of ~~the~~ marine aerosols in the offshore and pelagic regions.

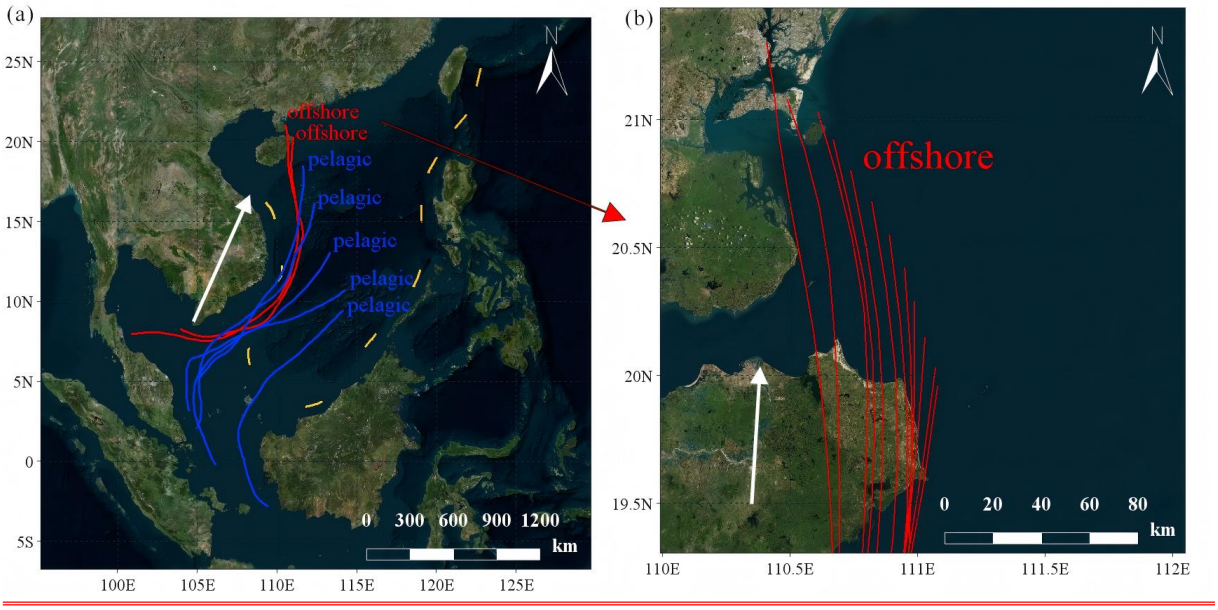

Fig. 6 (a) The 72-h backward trajectory air mass source traces in the offshore (red solid lines) and pelagic (blue solid lines) regions. (b) Detailed map of the backward trajectory air mass source traces passing through the mainland areas (© Google Earth). The white arrows represented the direction of air mass transport.

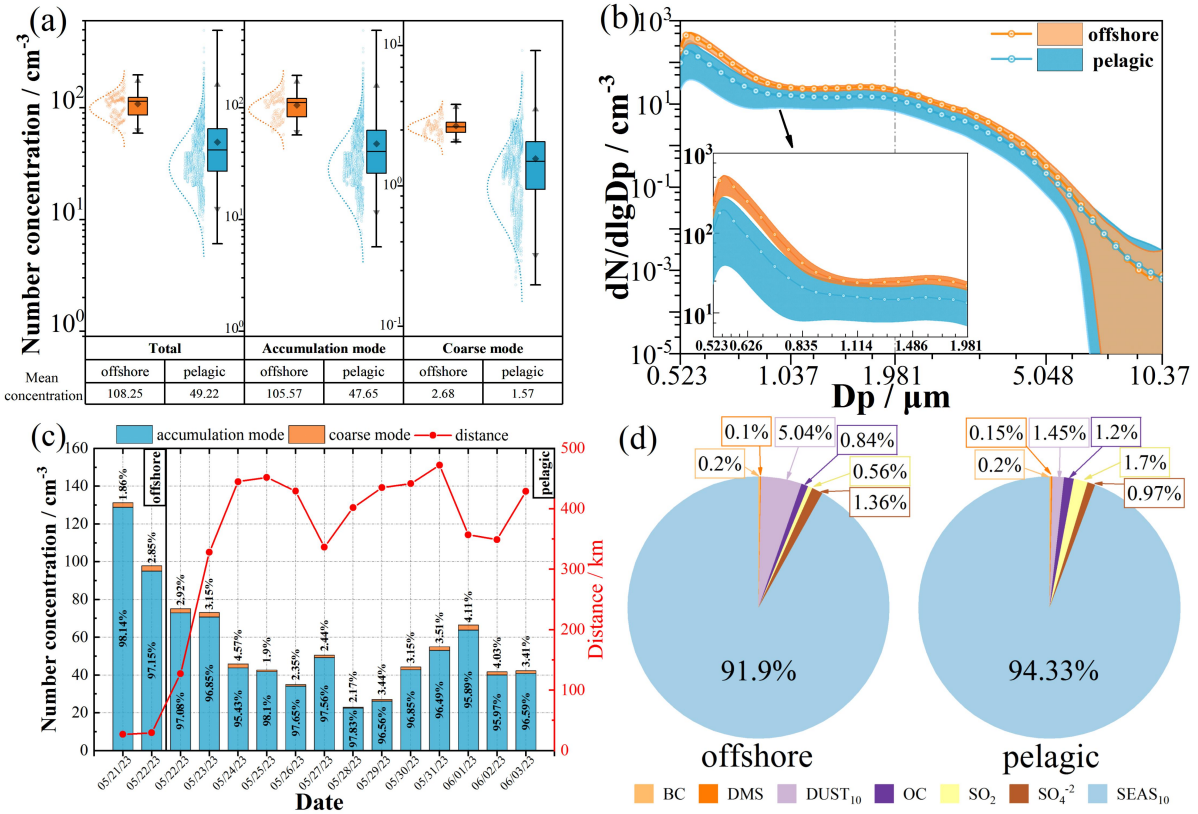
(a)
Number concentration / cm-3
Total
Accumulation mode
Coarse mode
Mean concentration
offshore
pelagic
108.25
49.22
105.57
47.65
2.68
1.57
(b)
dN/dlgDp / cm-3
offshore
pelagic
0.523
1.037
1.981
5.048
10.37
Dp / μm
(c)
accumulation mode
coarse mode
distance
Number concentration / cm-3
Distance / km
Date
(d)
0.1%
5.04%
0.84%
0.2%
0.56%
1.36%
91.9%
offshore
0.15%
1.45%
1.2%
0.2%
1.7%
0.97%
94.33%
pelagic
BC
DMS
DUST10
OC
SO2
SO4-2
SEAS10

480

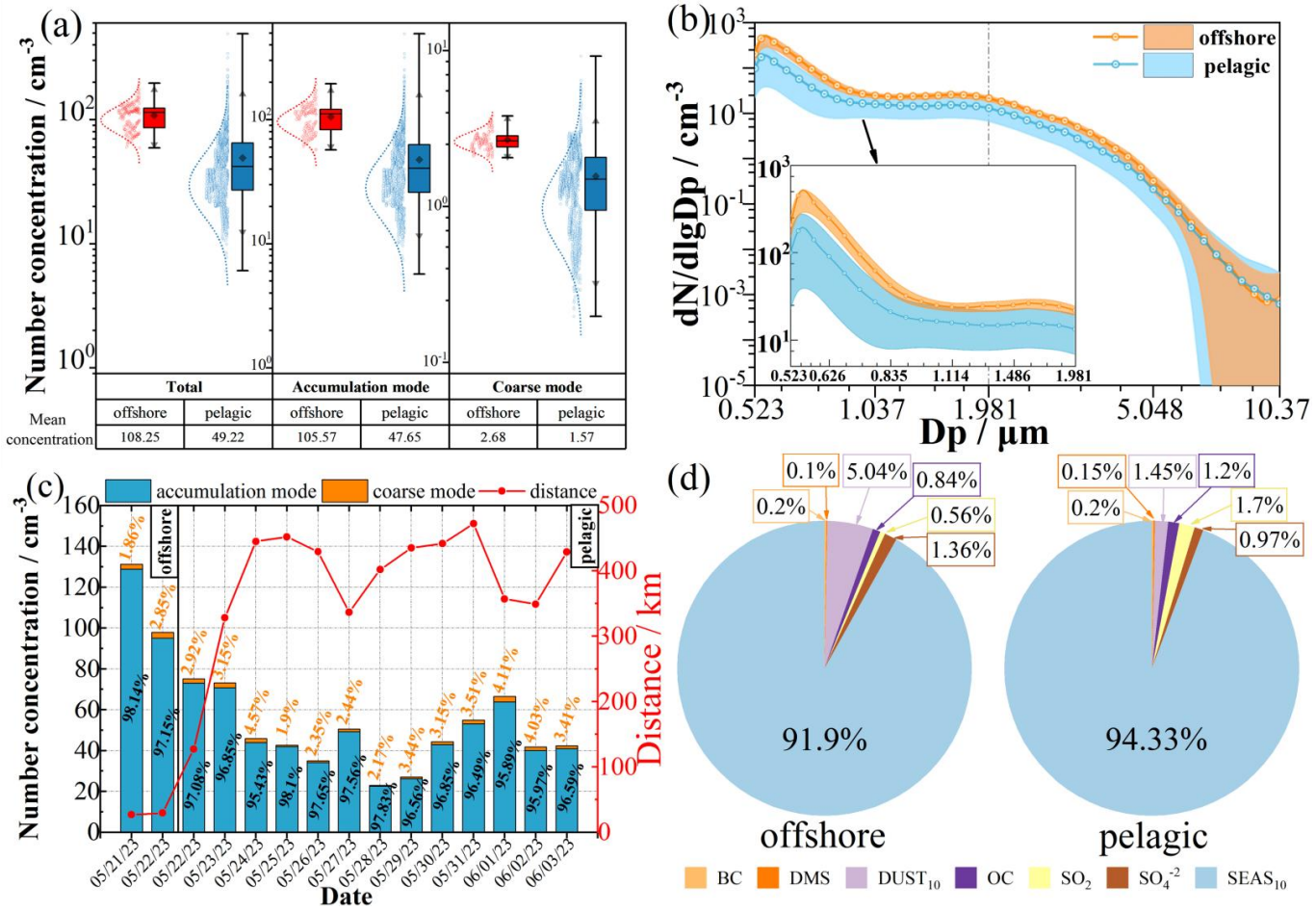

Fig. ~~7~~7 Classification of the shipboard observation path in the SCS: (a) Accumulation and coarse mode particle sizes graded NCs in the offshore and pelagic regions. For the box plots, the boxes represented the 25th to 75th percentile value, the black whisker represented the maximum and minimum range, the black triangle represented the 1.5 inter-quartile range, the black diamond marker represented the mean value, and the black horizontal line represented the median value. (b) The NCs of average size distributions (the solid lines and circles) and standard deviations (the shaded areas) for marine aerosols of 0.5 to 10 μm diameters in the offshore and pelagic regions. (c) The ~~diurna~~daily average~~l~~ variations of the proportions and the NCs of two aerosol particle modes were shown with the ~~distances from the coast~~distances from coast. (d) The distributions of marine aerosol components in the offshore and pelagic regions. The pie charts showed the average aerosol composition based on the mass concentrations from the Merra-2 aerosol dataset during the whole cruise period.

Table 3

Distributions of NCs for different aerosol particle modes in different ocean regions. Mean and SD, respectively, represent the mean values and standard deviations of the related meteorological parameters.

Observation Area	South China Sea			
Route Location	Offshore Region		Pelagic Region	
Marine Aerosol Parameters	Mean	SD	Mean	SD

Accumulation Mode (cm^{-3})	105.57	25.52	47.65	31.63
Coarse Mode (cm^{-3})	2.68	0.38	1.57	0.80
~~Total~~Total (cm^{-3})	108.25	25.43	49.22	31.97
Accumulation Mode / Total (%)	97.52	-	96.81	-
Coarse Mode / Total (%)	2.48	-	3.19	-
Meteorological Parameters				
WS ($m\ s^{-1}$)	10.74	1.95	8.64	3.70
RH (%)	91.20	1.72	82.41	3.40
T_{OBS} (℃)	28.19	0.57	29.18	0.87
SST (℃)	27.71	0.37	29.78	0.33

3.3. Diurnal variation of NCs and their affecting factors in pelagic regions

The results of Section 3.2 showed that ~~the~~ distributions and components of marine aerosols in different regions were influenced by ocean productions and ~~emissions, as well as~~ continental transports. Among them, ~~the~~ degree of impact on marine transport and background aerosols caused by continental transport and marine productiongeneration ~~sources~~ differ greatly due to ~~the~~ discrepancies in the degree of continental transport and marine biological activities at different ~~distances from the coast~~distances from coast. Beyond that, many meteorological parameters, such as WS, T2m, SST, and SST-T_{2m}, might influence concentration and distribution of marine aerosols. It is expected that there are diurnal differences. ~~Beyond that, on the one hand, many meteorological parameters, such as WS, T_{2m}, SST, and SST-T_{2m}, might influence the concentration and distribution of marine aerosols. On the other hand, the meteorological parameters had obvious day-night differences.~~ Therefore, we analyzed the diurnal variations of ~~the~~ NCs and the correlations between ~~the~~ NCs and different meteorological parameters in this section. In pelagic regions, ~~In that t~~the sources of 72-h backward trajectory air masses were from the ocean, and observational data were processed to~~, we selected those marine aerosol data in the pelagic areas with total marine aerosol NCs not exceeding 120 cm^{-3}~~ ~~to~~ exclude~~de~~ the ~~the influence of~~ continental ~~transport~~influence. These aerosol data ~~also~~ conformed to ~~the classification method~~clean marine periods, which were~~as~~ proposed by Saliba (2019) to extract relatively clean marine aerosol data; ~~meanwhile,~~ these NCs thus distinctly represented the characteristics of ~~the~~ local productiongeneration of marine aerosol in these regions.

Fig. 9~~8~~a showed ~~the~~ diurnal variations of the ~~total~~ mean values of total NCs in the pelagic region. To better compare the diurnal variation, we divided the data into different periods according to sunrise and sunset times. Consequently, we selected the sunrise and sunset moments, along with the surrounding one-hour interval, as the transition periods to eliminate the effects of day-to-night transitions. Fig. 9~~8~~a showed ~~a~~ a clear diurnal variation trend~~clear diurnal variation emerged~~. For accumulation mode,~~The variations became readily visible for the accumulation mode, following a definite pattern:~~ the NCs remained falling trend in the nighttime (00:00-03:00 and 21:00-23:00 LT), and they began steadily rising in the night-to-day transition (NDT) period (04:00-06:00 LT). Then they ~~remained~~showed a slightly upward~~rising or falling~~ in the daytime

(07:00-17:00 LT), but began to fall steadily in the day-to-night transition (DNT) period (18:00-20:00 LT). ~~Meanwhile, w~~We also found that ~~the~~ NCs ~~had~~exhibited apparent discrepancies between the daytime and nighttime, and ~~they~~tended to increased or decreased significantly during the transition periods.

~~The c~~Comparisons of ~~the~~ size distributions (Fig. ~~9~~8b) showed that number size distributions exhibit a relatively stable value in 0.835-1.981 μm particle size range, and subtle differences emerged in this particle range. Quantitatively, peak diameter varied slightly across periods: 0.571 μm in nighttime, 0.567 μm in the NDT period, 0.569 μm in daytime, and 0.570 μm in the DNT period. More notably, the peak value was 147.05 cm^{-3} in nighttime, then rose to 155.87 cm^{-3} in NDT period, further increased to 165.60 cm^{-3} in daytime, and reached the highest value of 206.79 cm^{-3} in DNT period, registering a 0.4-fold increase relative to the nighttime baseline. The peak value showed a clear and continuous increasing trend, which may reveal variations in aerosol production. ~~the NCs of the different periods were evenly distributed in the 0.5 to 2.0 μm diameter range.~~ In addition, ~~the~~ all ~~average~~ size distributions for marine aerosols had the same shape. ~~were consistent. The reason for these phenomena was~~The consistent shape can be explained by their common marine origin and production mechanisms. ~~that almost all relatively clean marine aerosols were from the oceans.~~ The NCs of ~~the~~ different aerosol particle modes in ~~the~~ different periods were counted in Fig. ~~9~~8c, and we can find that ~~the~~ average total NCs ~~of the total marine aerosols~~ were significantly different in different periods. Specifically, the ~~total~~total NC was ~~43.86~~44.03 cm^{-3} in the nighttime, and 47.~~06~~5 cm^{-3} in the first transition period (i.e.~~,~~ NDT), but it was ~~48.99~~49.28 cm^{-3} in the daytime, and reached the highest (~~58.56~~59.59 cm^{-3}) in the second transition period (i.e.~~,~~ DNT). The differences were all statistically significant ($p < 0.01$). The comparisons of the accumulation modes were consistent with those of the total~~total~~ NCs. The NC of the accumulation mode was 42.~~26~~43 cm^{-3} in the nighttime, 45.~~90~~47 cm^{-3} in the NDT period, 47.~~62~~33 cm^{-3} in the daytime, and 5~~7~~6.~~91~~89 cm^{-3} in the DNT period. The differences were also statistically significant ($p < 0.01$). There were pronounced diurnal NC variations, with maximum differences of 35% observed between daytime, nighttime, and transition periods. However, there were no significant differences in the NCs of the coarse modes between different periods, as mentioned above, which were 1.60 cm^{-3}, 1.58 cm^{-3}, 1.66 cm^{-3}, and 1.68 cm^{-3}, respectively.

To explore the reasons for these differences, we further analyzed the correlation coefficients between the NCs and the meteorological parameters (Fig. ~~10~~9a)~~, suggesting that the NCs of all aerosol particle modes have positive correlations to the WSs.~~ ~~The c~~Correlation coefficients were 0.41 for ~~the~~ coarse mode, 0.57 for ~~the~~ accumulation mode, and 0.58 for ~~the total modes~~total NCs. This correlation suggested that the NCs of all aerosol particle modes have positive correlations to the WSs. ~~On the contrary~~By contrast, negative correlations between SST and NC were found, which were~~are~~ -0.24, -0.45, and -0.47, respectively, and the NCs were low in the time periods with high SST. Compared to the WS and SST, our results showed that ~~the~~ SST-T_{2m} has a ~~more significant~~ negative correlation with ~~the~~ NCs, with correlation coefficients of -0.30, -0.82, and -0.83. Fig. ~~10~~9b showed that ~~the~~ WS was lower during ~~the~~ nighttime, and ~~the~~ SST and SST-T_{2m} values were ~~greater~~higher, resulting in NCs lower than those in daytime~~so the NCs were lower than those in the daytime~~. In the NDT period, ~~the~~ WS did not change significantly, but an obvious decrease in the SST and SST-T_{2m} was found, ultimately resulting in a noticeable increase in ~~the~~ NCs. In this period, ~~the~~ SST and SST-T_{2m} were the dominant factors. However, in the DNT period, ~~the~~ NCs

were highest due to the lowest values of SST and SST-T_{2m} and the highest WS. In this period, the significant reduction in WS led to a decrease in ~~the~~ NCs. From the above analysis, the meteorological parameters have a joint impact on the production and distribution of marine aerosols.

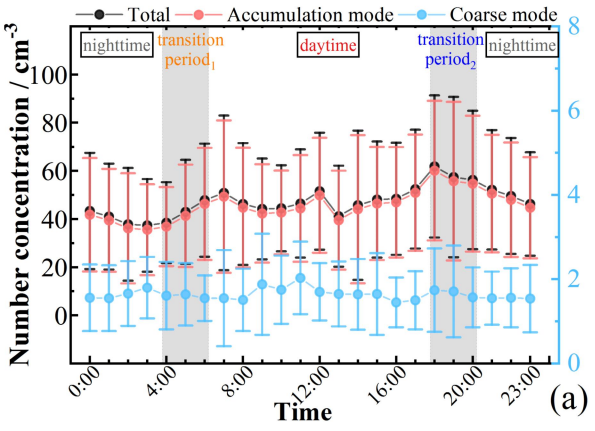

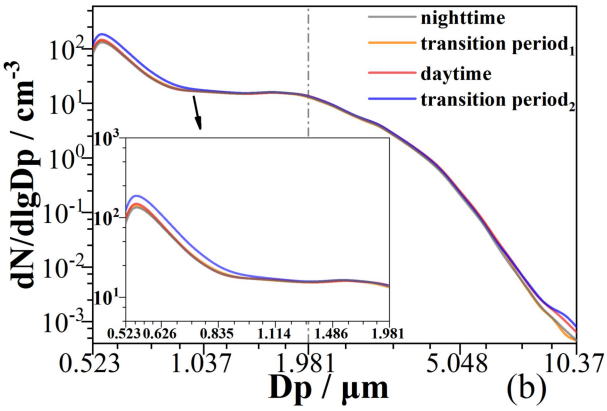

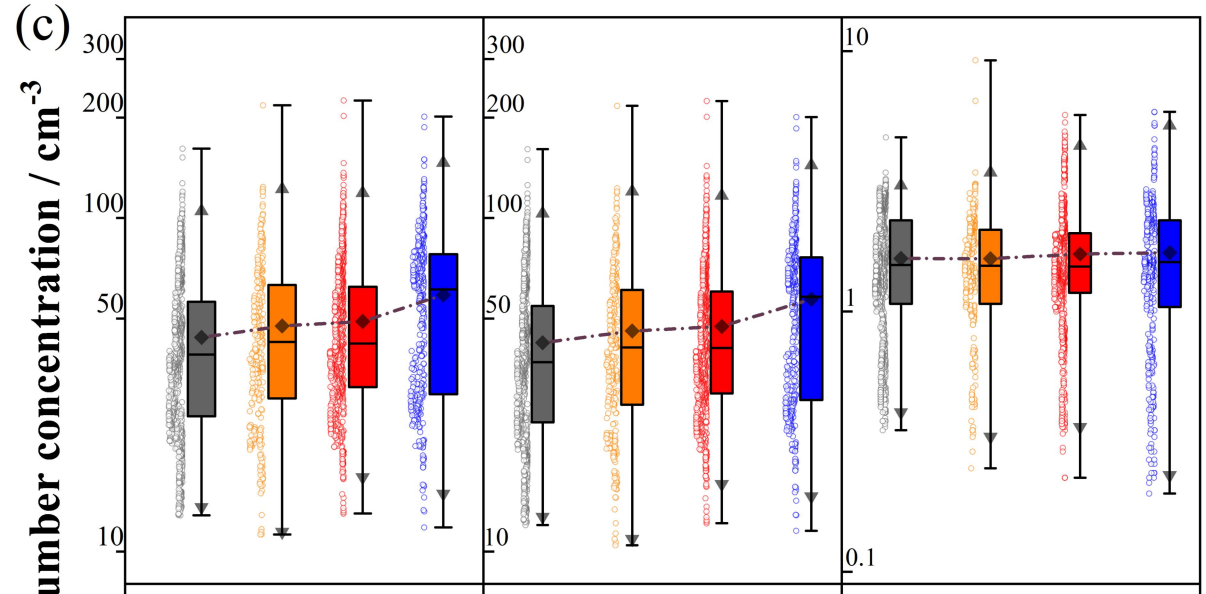

	Total				Accumulation mode				Coarse mode			
	nighttime	transition period$_1$	daytime	transition period$_2$	nighttime	transition period$_1$	daytime	transition period$_2$	nighttime	transition period$_1$	daytime	transition period$_2$
Mean concentration	44.03	47.5	49.28	59.59	42.43	45.90	47.62	57.91	1.6	1.60	1.66	1.68

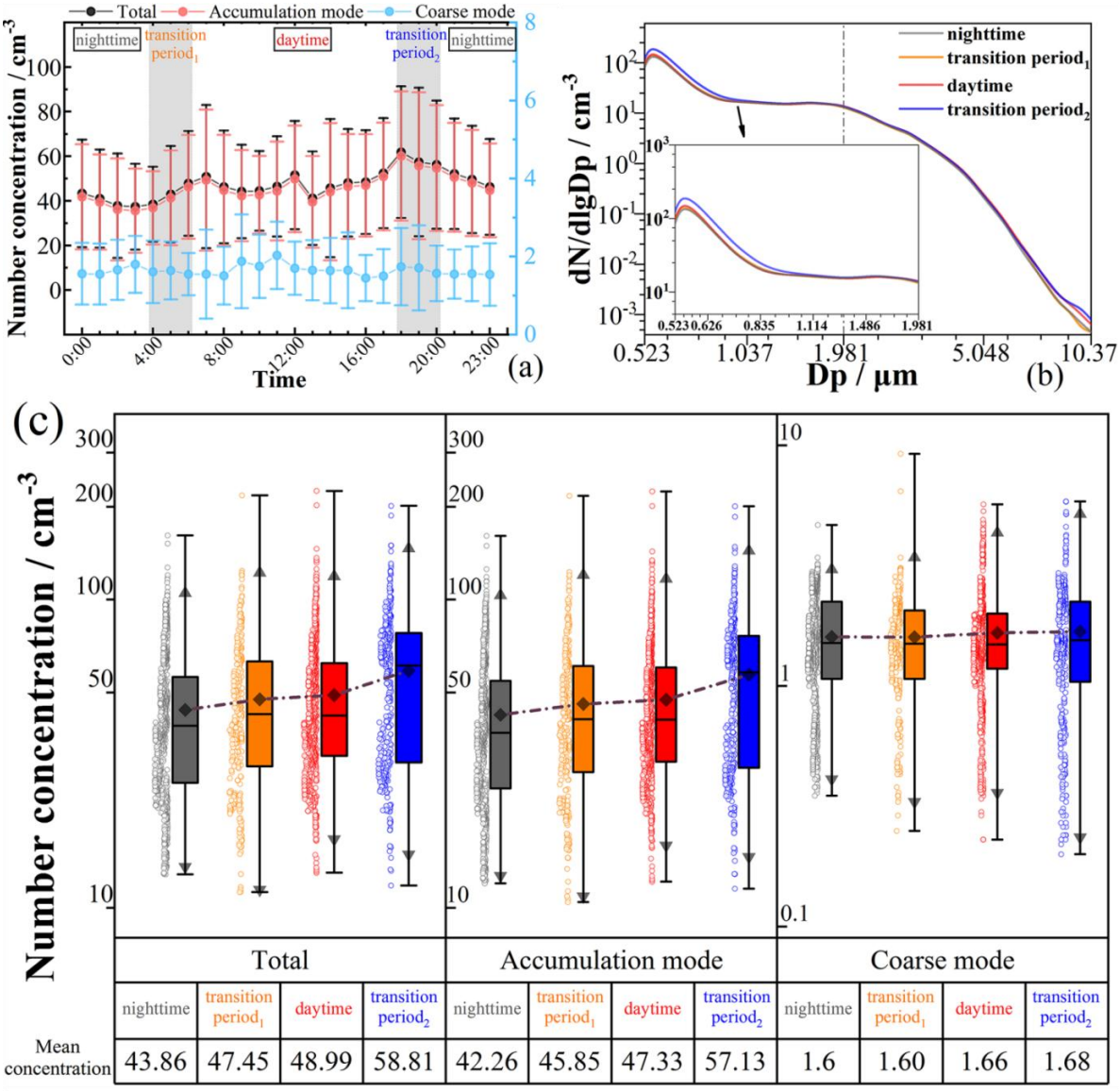

555

Fig. ~~9~~8 (a) Diurnal variations of the total mean values of the NCs in the different aerosol particle modes. The vertical bars showed the standard errors (the shadow areas represented the transition periods between daytime and nighttime). (b) The NCs of average size distributions for marine aerosols of 0.5 to 10 μm diameters in different time periods. (c) The NCs of the different aerosol particle modes in different time periods. For the box plots, the boxes represented the 25th to 75th percentile value, the black whisker represented the maximum and minimum range, the black triangle represented the 1.5 inter-quartile range, the black diamond marker represented the mean value, and the black horizontal line represented the median value.

560

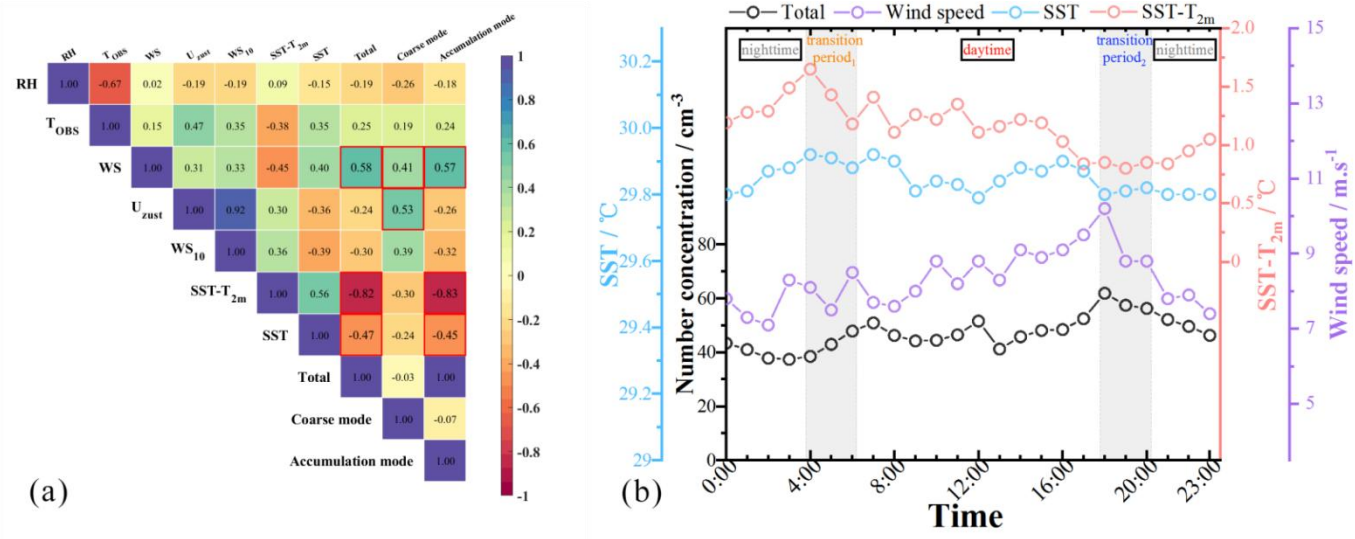

Fig. ~~10~~9 (a) The correlation coefficients between the NCs of all aerosol particle modes and different meteorological parameters. Correlation plot showing the Pearson correlation values of all marine aerosol NCs and meteorological parameters measured in pelagic regions. (b) The comparisons between the diurnal variations of ~~total~~total NCs, SST, SST-T_{2m}, and WS.

3.3.1. Influence of the WS on marine aerosol NCs

Our measurement results provided robust evidence for ~~the~~ wind-driven marine aerosol production mechanism in the pelagic region. In all SST intervals, we ~~can~~ observed ~~an~~ ~~obvious~~ positive correlation between ~~the~~ WS and ~~the~~ NCs of all aerosol particle modes (Fig. ~~11~~10), with R values greater than 0.8. In the pelagic region, the NCs were strongly influenced by the local production~~s~~ and marine aerosols had a relatively short lifetime. Under the influence of sea surface wind, the ocean wave fluctuations increased~~; meanwhile~~, and the friction at the sea surface intensified with wind stresses~~the frictions of the sea surface intensified with the actions of the wind stresses~~. The air bubbles generated and ~~existed~~present on the sea surface, which subsequently ruptured to form numerous ~~lots of~~ water droplets, eventually~~and then~~ produc~~ed~~ ~~the~~ primary marine aerosol after evaporation and crystallization processes (Blanchard et al., 1980; Saliba et al., 2019). Therefore, increased WS both intensified bubble rupture by enhancing sea surface friction and promoted air-sea gas transfer (Jaeglé et al., 2011; Mårtensson et al., 2003). This increased activity elevated the production of marine aerosols and natural marine precursors, ultimately raising the NCs in the pelagic region.~~Therefore, under the WS increased accompanied by synergistic influences of the gas-to-particle conversion and sea surface wind physical friction, the NCs increased in the pelagic region.~~

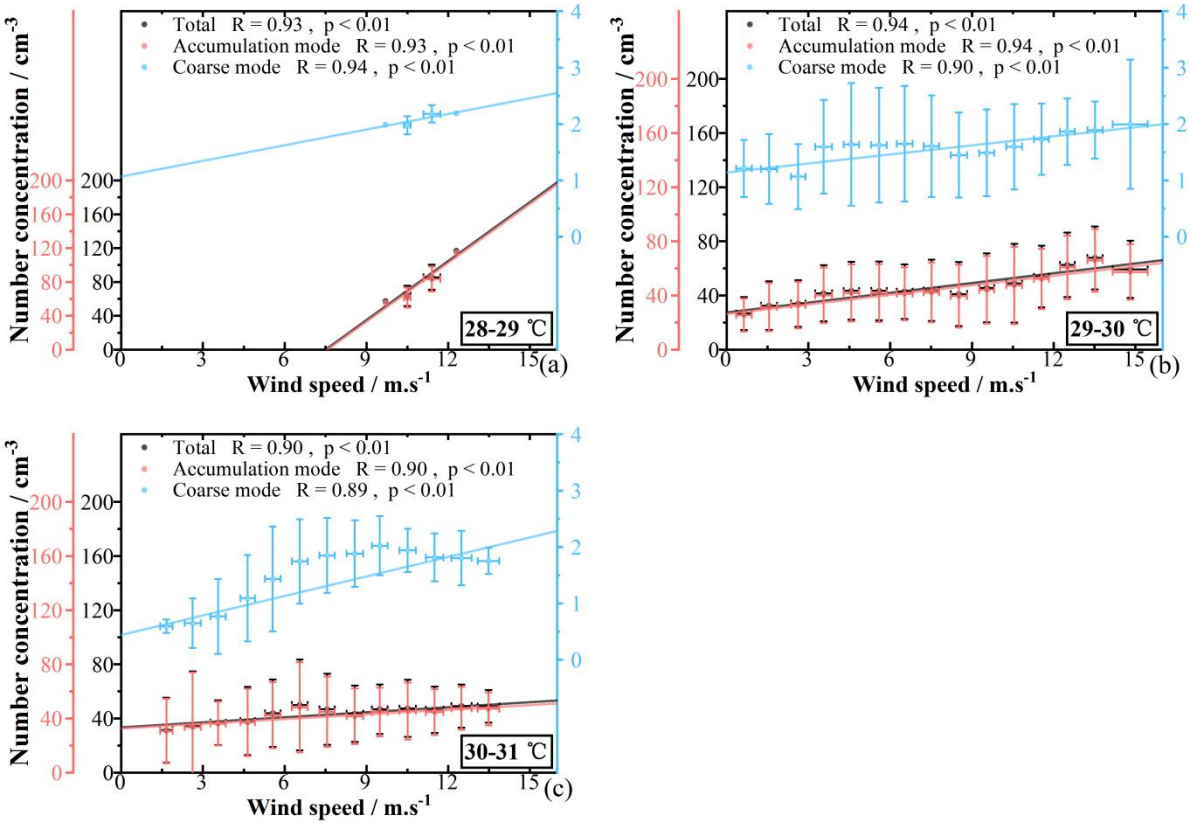
Total R = 0.93 , p < 0.01
Accumulation mode R = 0.93 , p < 0.01
Coarse mode R = 0.94 , p < 0.01
28-29 ℃
(a)
Total R = 0.94 , p < 0.01
Accumulation mode R = 0.94 , p < 0.01
Coarse mode R = 0.90 , p < 0.01
29-30 ℃
(b)
Total R = 0.90 , p < 0.01
Accumulation mode R = 0.90 , p < 0.01
Coarse mode R = 0.89 , p < 0.01
30-31 ℃
(c)
Number concentration / cm-3
Wind speed / m.s-1

580

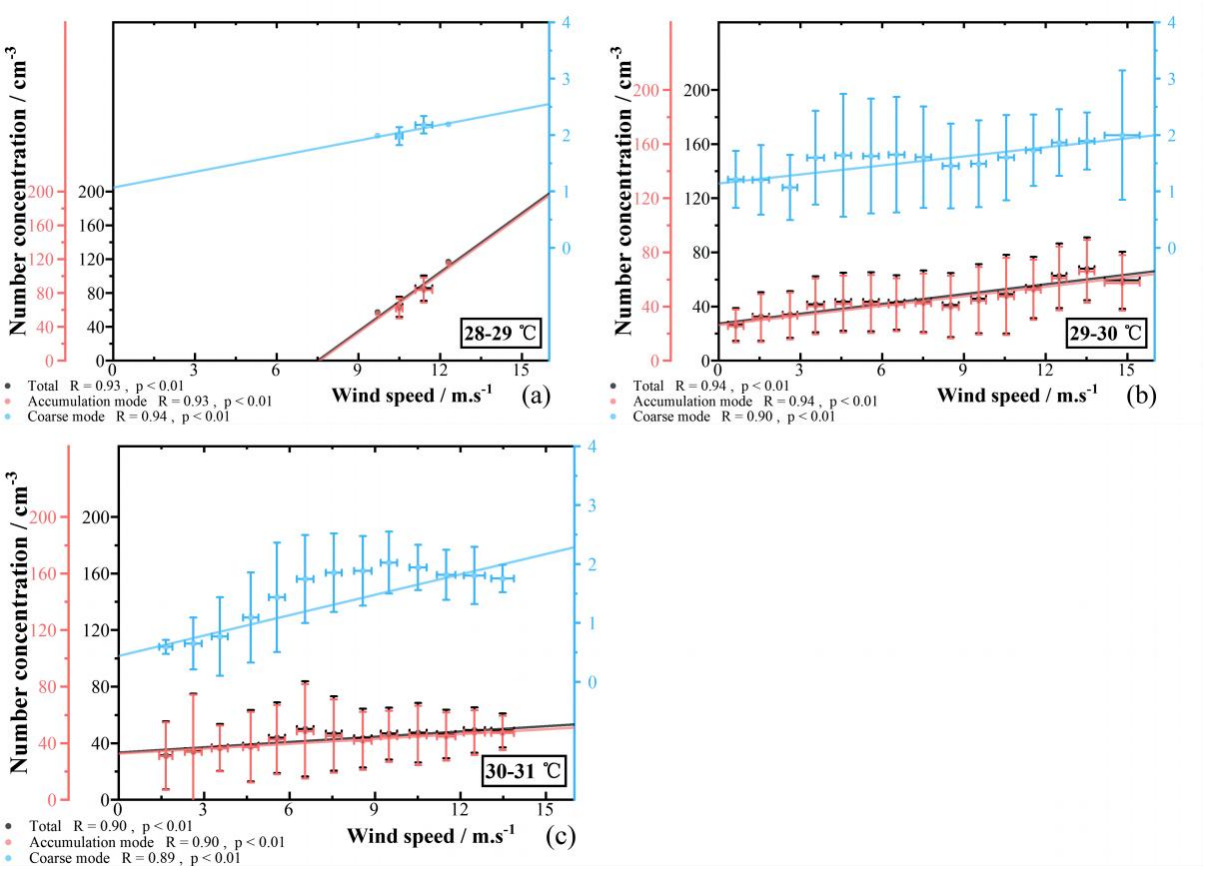

Fig. ~~11~~10 The NCs versus WS in the pelagic region. The NC of all aerosol particle modes versus WS for 28-29 ℃ (a), 29-30 ℃ (b), and 30-31 ℃ (c) SST intervals. The error bars represented the standard deviations. The R represented the Pearson correlation coefficients, and the p values were performed to test whether the correlations were significant.

585

3.3.2. Influence of the SST and SST-T_{2m} on marine aerosol NCs

Although ~~the~~ WS can partly explain the variability of ~~the~~ NCs, ~~the~~ NCs exhibited a ~~more obvious~~ negative dependence on SST in all WS intervals. To analyze how SST influenced ~~the~~ NCs in the pelagic region, Fig. ~~12~~S4 showed the NCs of all aerosol particle modes versus SST (28 ℃ ≤ SST ≤ 31 ℃) in the WS intervals, in which ~~the~~ WS was approximately constant.
590 The design~~It~~ may largely exclude the influences of ~~the~~ WS on ~~the~~ NC. A negative correlation existed between ~~We found a negative correlation between the~~ SST and ~~the~~ NCs for ~~the~~ WS of 0-15 m s^{-1} in the SCS, with all their R values being ~~all~~ more negative than~~smaller than~~ -0.75 (Fig. ~~12~~S4). By comparing regression slopes across the different aerosol particle modes, ~~With the comparisons of the regression slopes across the different aerosol particle modes, tthe SST was likely more sensitive to the accumulation mode~~he accumulation mode was likely more sensitive to SST. Thise observed trend~~result~~ was
595 inconsistent with some laboratory studies (Keene et al., 2017; Forestieri et al., 2018) ~~consistent with the previous studies~~

~~(Salter et al., 2014; Zábori et al., 2012b)~~ but~~ consistent with the previous studies (Salter et al., 2014; Zábori et al., 2012b)~~~~inconsistent with some laboratory studies (Keene et al., 2017; Forestieri et al., 2018).~~ ~~However, a~~A recent study also reported~~showed~~ ~~decreasing that the~~ NCs ~~decreased~~ with rising~~the~~ SST (Christiansen et al., 2019).~~ These comparisons suggested that the influences of the SST on the NCs might be different in different seas due to the different components of the seawater.~~ In ~~the~~ pelagic region of the SCS, combined evidence from prior studies (Christiansen et al., 2019; Salter et al., 2014; Zábori et al., 2012b) and our observational trends suggested that elevated SST may suppress near-surface air entrainment volumes, consequently decreasing plunging jets.~~according to the results of the previous studies and this study, we inferred that the volume of the air entrained might have decreased as the SST was increased, resulting in the decrease of the plunging jet.~~ Meanwhile, the processes of the bubble rupture changed; the larger central bubbles (the primary bubbles rising to the sea surface) ruptured at the sea surface, small daughter bubbles (secondary bubbles with smaller diameters, generated at the edges of central bubbles) were produced. Theses daughter bubbles are critical for formation of submicron marine aerosols (Miguet et al., 2021; Sellegri et al., 2023). ~~the daughter bubbles of smaller diameters were generated at the edges of the central bubbles when the central bubbles ruptured at the sea surface.~~ The ~~The g~~generations of ~~the~~ daughter bubbles decreased with an~~the~~ increasing ratio of seawater density to viscosity and ~~the~~a decreasing ratio of seawater viscosity to surface tension.~~;~~ Under increasing SST,~~however,~~ the ratio of seawater density to viscosity might increase and the ratio of seawater viscosity to surface tension might decrease~~ under the increasing SST~~, and the number of ~~the~~ sea surface bubbles might decrease (Miguet et al., 2021; Sellegri et al., 2023). Therefore, these factors might ultimately result in decreased marine aerosol NCs, especially for the accumulation ~~aerosol~~ mode, with the increasing SST in the SCS.

Compared to the WS and SST, ~~the~~ SST-T_{2m} can better reflect the variations of the NCs ($R > 0.90$, Fig. ~~13~~11). Meanwhile, the correlations can explain that ~~Fig. 13 indicated that the~~ NCs had a significant negative correlation with the SST-T_{2m} (-1 °C ≤ SST ≤ 4 °C).~~.~~ Figs. S5~~13~~ and S6~~14~~ illustrated the NC of all aerosol particle modes versus SST-T_{2m} respectively ~~in~~for ~~the~~ WS and SST intervals, and further presented this negative correlation under controlled WS and SST intervals. ~~respectively.~~ Prior studies (Lewis et al., 2004; Yuan et al., 2019) had suggested that SST-T_{2m} may be related to atmospheric stability and play a role in air convection, mechanical mixing over the ocean, and plume rise processes. Song et al. (2023) had also indicated that SST-T_{2m} influence marine aerosol production by affecting atmospheric stability and thus the interfacial and effective production fluxes of marine aerosols by affecting the sea state, sea wave, and the process of the whitecap formation. Combining these previous inferences with our observational negative correlation between SST-T_{2m} and NCs, it was plausible that SST-T_{2m} could influence marine aerosol transport (e.g. potential upward transport driven by plume rise) and production. For example, increased SST-T_{2m} may intensify plume rise, leading to reduced NCs near the sea surface. Additionally, increased SST-T_{2m} might indirectly decrease aerosol production by altering atmospheric stability. ~~In the WS and SST intervals, we found a significant negative correlation between the SST-T_{2m} and the NCs in the SCS (Fig. 14). The SST-T_{2m} was the major determinant of the atmospheric stability, simultaneously playing a relatively important role in the processes of the air convection and mechanical mixing over the ocean (Lewis et al., 2004). With increased SST-T_{2m}, the plume rise phenomenon and the upward transport of marine aerosols might intensify (Yuan et al., 2019). The gravity had little influence~~

~~on the vertical motion of the small marine aerosol particles; for instance, the marine aerosols with 1 μm diameters needed nearly 24 hours to fall 10 meters in the still air. Hence, the NCs may decrease on the sea surface due to vertical transport. Moreover, the SST-T_{2m} probably influenced the marine aerosol generation by affecting atmospheric stability and thus the interfacial and effective production fluxes of marine aerosols by affecting the sea state, sea wave, and the process of the whitecap formation (Lewis et al., 2004; Song et al., 2023).~~ These phenomena might be an important factor affecting the differences in the marine aerosol NC distributions; meanwhile, they might be important for the abovementioned different conclusions of the previous studies on the relationship between the SST and NCs. The differences in the SST-T_{2m} might cause the inter-study differences despite the consistent SST during the experiment. The specific reasons needed to be further proved by the subsequent targeted research. In summary, the SST-T_{2m} might influence the marine aerosol transport and production~~generation~~ processes, resulting in differences in NCs. Hence, the SST-T_{2m} may be a new and significant parameter to better quantify the impact on the marine aerosol transport~~s~~ and production~~generations~~ in the SCS.

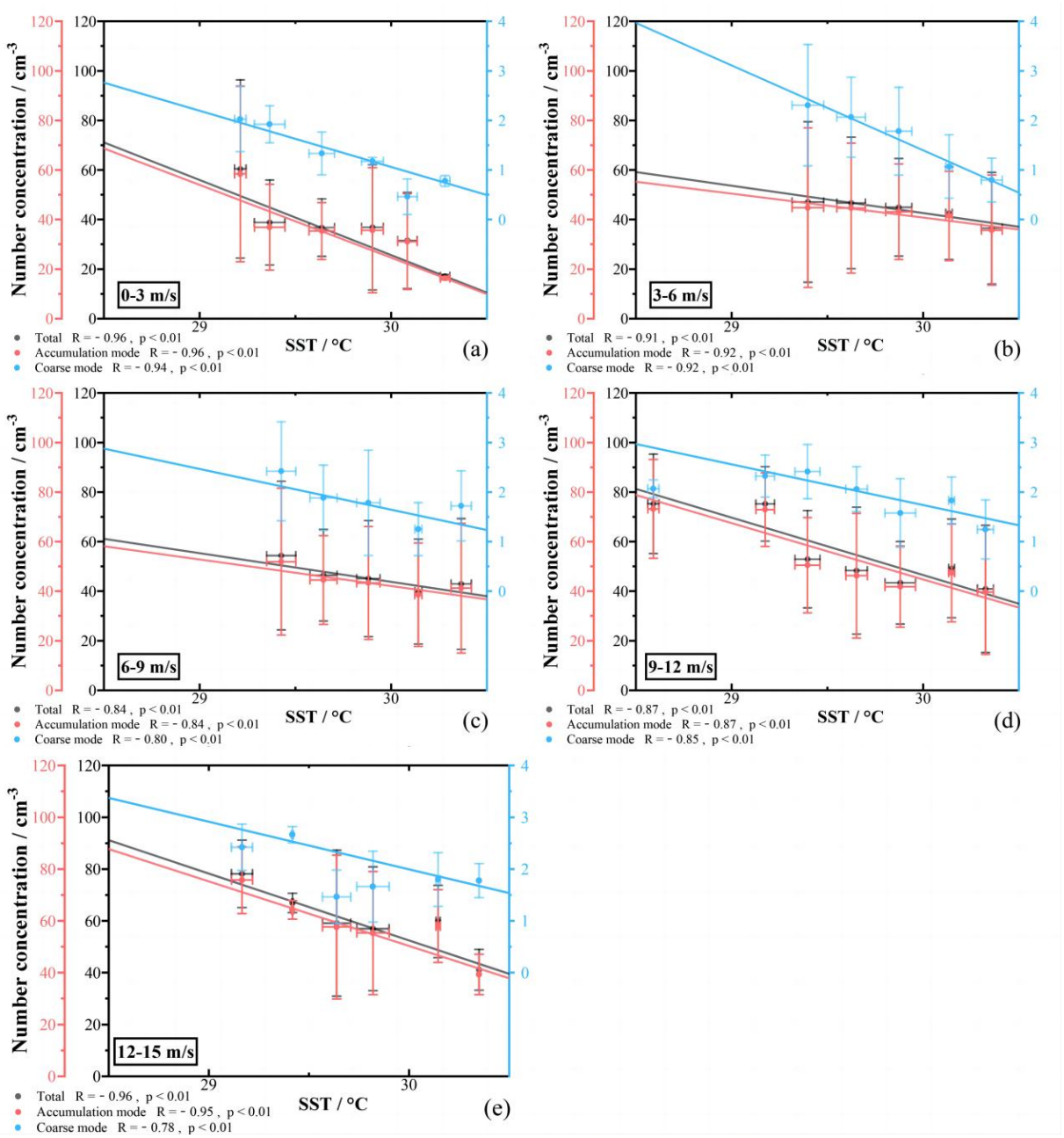

Fig. 12 The NCs versus SST in the pelagic region. The NC of all aerosol particle modes versus SST for 0-3 m s^{-1} (a), 3-6 m s^{-1} (b), 6-9 m s^{-1} (c), 9-12 m s^{-1} (d), and 12-15 m s^{-1} (e) WS intervals. The error bars represented the standard deviations. The R represented the Pearson correlation coefficients, and the p values were performed to test whether the correlations were significant.

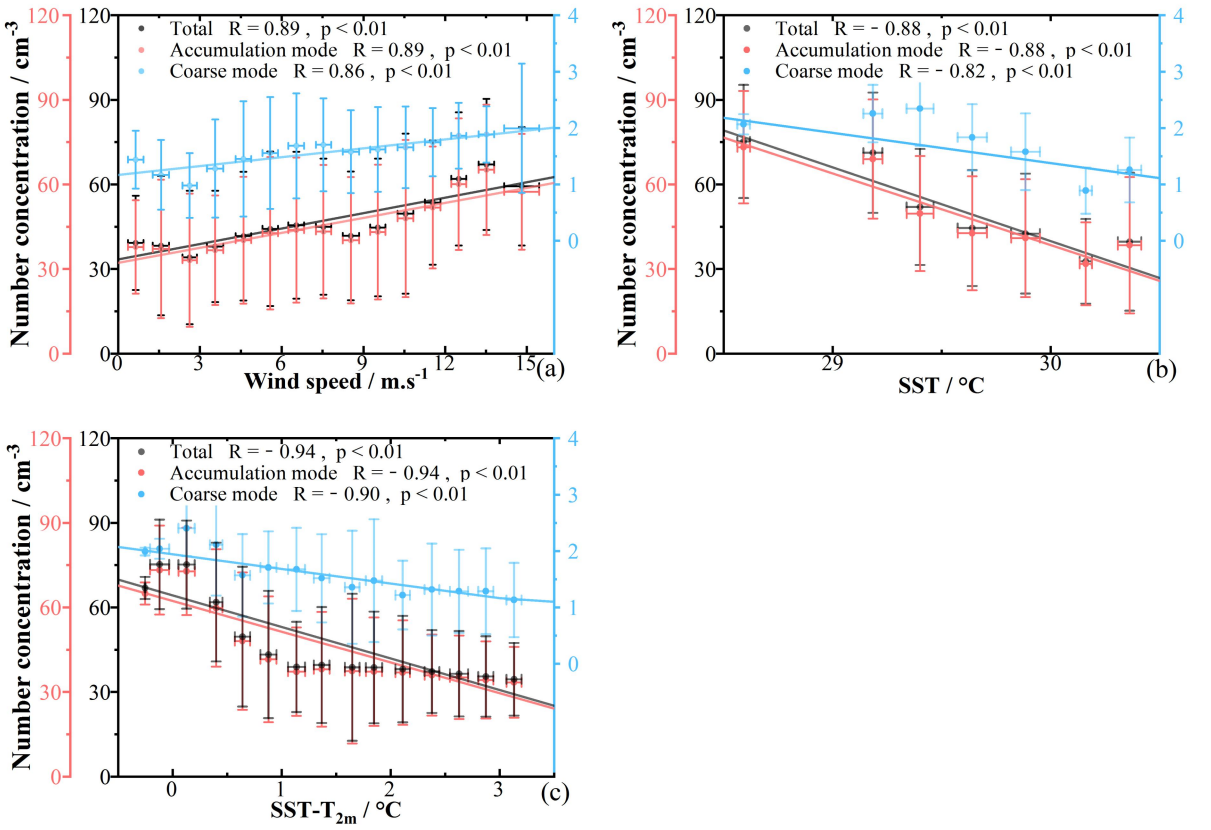
Total R = 0.89 , p < 0.01
Accumulation mode R = 0.89 , p < 0.01
Coarse mode R = 0.86 , p < 0.01
Number concentration / cm-3
Wind speed / m.s-1
(a)
Total R = - 0.88 , p < 0.01
Accumulation mode R = - 0.88 , p < 0.01
Coarse mode R = - 0.82 , p < 0.01
Number concentration / cm-3
SST / °C
(b)
Total R = - 0.94 , p < 0.01
Accumulation mode R = - 0.94 , p < 0.01
Coarse mode R = - 0.90 , p < 0.01
Number concentration / cm-3
SST-T2m / °C
(c)

645

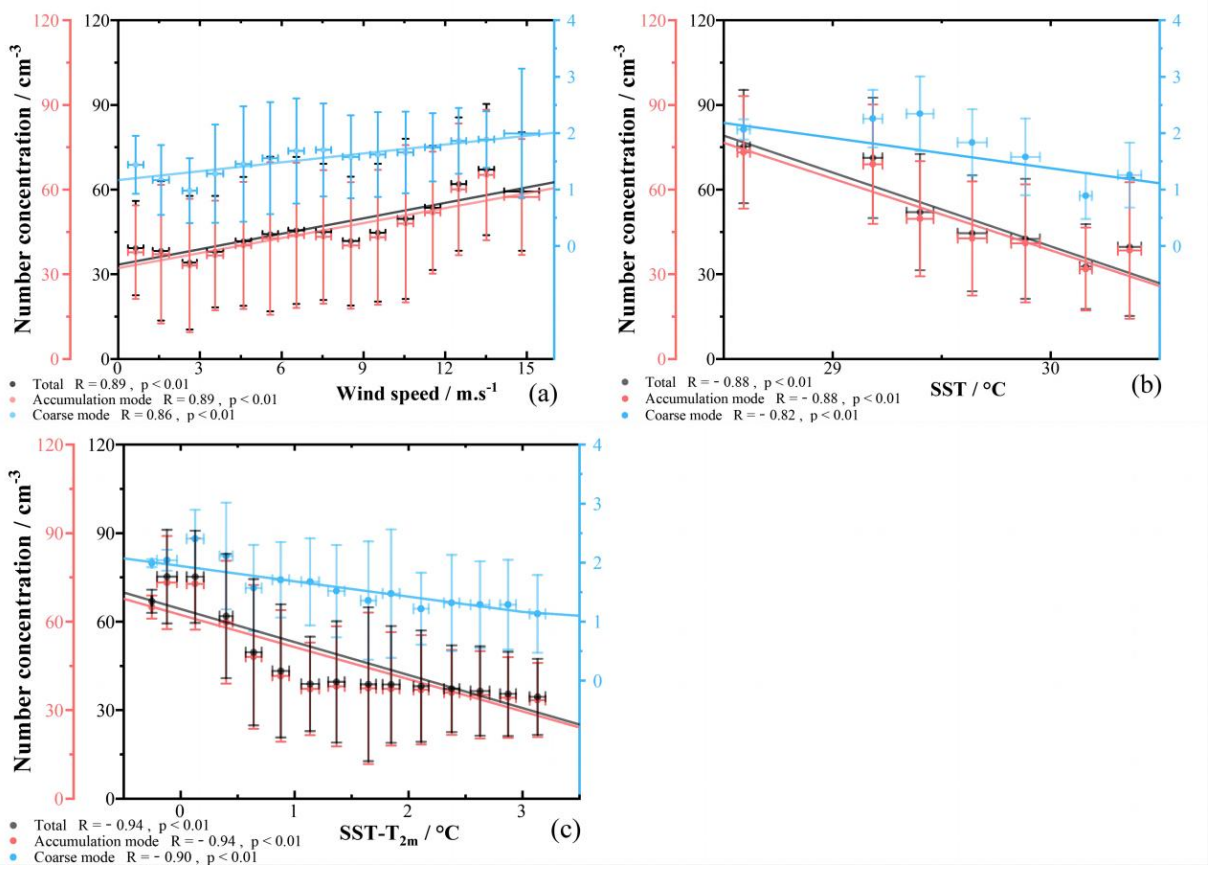

Fig. ~~13~~11 The relationship between the NC of all aerosol particle modes and WS (a), SST (b), and SST-T_{2m} (c). The error bars represented the standard deviations. The R represented the Pearson correlation coefficients, and the p values were performed to test whether the correlations were significant.

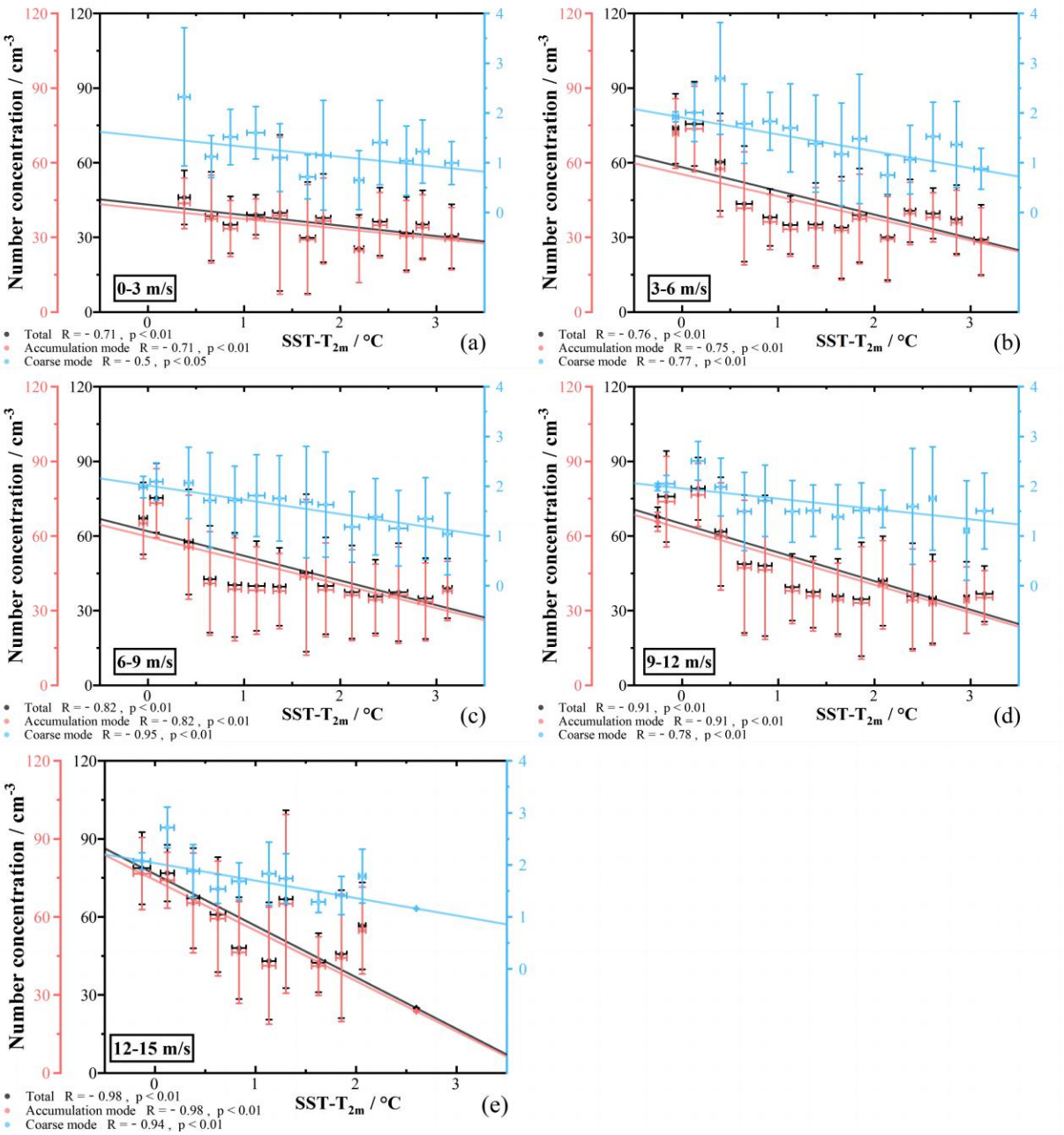

650 **~~Fig. 14 The NCs versus SST-T_{2m} in the pelagic region. The NC of all aerosol particle modes versus SST-T_{2m} for 0-3 m s^{-1} (a), 3-6 m s^{-1} (b), 6-9 m s^{-1} (c), 9-12 m s^{-1} (d), and 12-15 m s^{-1} (e) WS intervals. The error bars represented the standard deviations. The R represented the Pearson correlation coefficients, and the p values were performed to test whether the correlations were significant.~~**

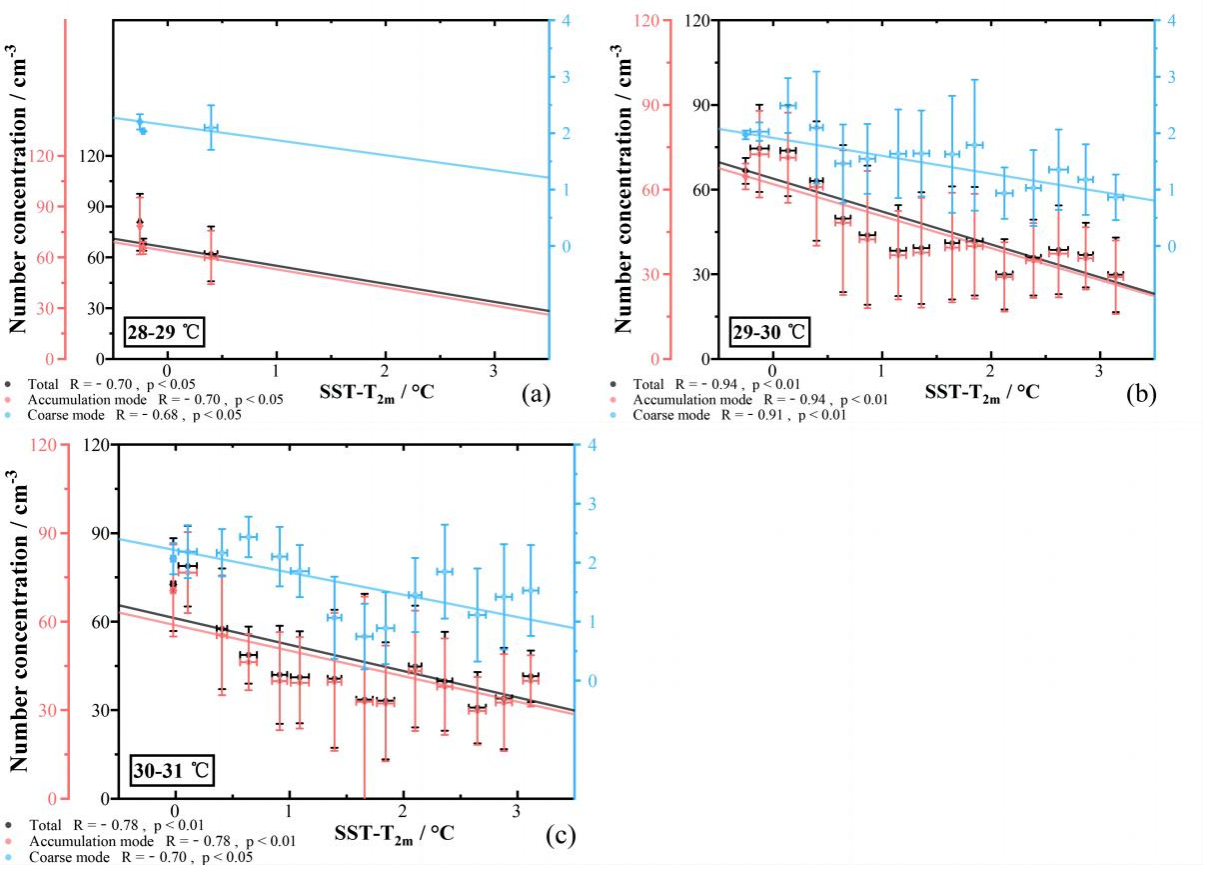

655 ~~**Fig. 15 The NCs versus SST-T_{2m} in the pelagic region. The NC of all aerosol particle modes versus SST-T_{2m} for 28-29 °C (a), 29-30 °C (b), and 30-31 °C (c) SST intervals. The error bars represented the standard deviations. The R represented the Pearson correlation coefficients, and the p values were performed to test whether the correlations were significant.**~~

4. Conclusions

This study utilized cruise-based observational data collected from 21 May to 15 June 2023 to examine marine aerosol NCs
660 and components within the data-sparse SCS. Measurements revealed ~~NCs for the total,~~ accumulation mode, ~~and~~ coarse mode~~s~~, and summed NCs of ~~54.01 ± 35.37 cm^{-3},~~ 52.35 ± 34.96 cm^{-3}, ~~and~~ 1.66 ± 0.83 cm^{-3}, and 54.01 ± 35.37 cm^{-3}~~,~~, respectively. Analysis of marine aerosol size distributions (Dp < 10.37 μm~~0.5–10 μm diameter~~) exhibited a bimodal structure, with modes at 0.542 μm and 1.981 μm. Spatial characterization of NCs and aerosol components between offshore and pelagic regions revealed distinct differences, demonstrating that distance from the coast significantly influences distributions
665 due to variations in aerosol transport and ~~generation~~production. Furthermore, meteorological parameters, particularly SST-T_{2m}, were shown to~~proved to~~ potentially induce changes in ~~the~~ aerosol transport and production~~generation processes~~, ultimately leading to discrepancies in ~~the~~ NCs. Diurnal cycles in meteorological parameters also drove pronounced aerosol

NCs variations, especially during daytime-nighttime transitions. Collectively, these findings proved to be key explanations of spatiotemporal marine aerosol variations in the SCS and theirthe potential affectinginfluencing factors.

The results obtained in the SCS demonstrated that the distributions of marine aerosol NCs and components depended on the distances from the coast. In offshore regions, aerosol components were strongly influenced by anthropogenic activities and continental transport processes, with both elevated NCs and higher proportions of continental aerosol components ($DUST_{10}$) compared to pelagic regions. Furthermore, NCs exhibited a negative correlation with distance from the coast, and this trend was consistent with diminishing continental aerosol contributions. Conversely, marine-derived components ($SEAS_{10}$ and DMS) dominated in pelagic regions, reflecting intensified marine aerosol production mechanisms.

The influences of meteorological parameters on marine aerosols differed in the pelagic regions. Increasing sea surface wind speed (WS) likely drove ocean wave fluctuations and heightened sea surface friction, promoting aerosol particle productiongeneration. Conversely, rising sea surface temperature (SST) could reduce plunging jet intensity and entrapped air volume, thereby potentially altering bubble rupture processes and decreasing NCs. Notably, the SST-T_{2m} anomaly exhibited the strongest correlation with NCs. Higher SST-T_{2m} likely reduced interfacial and effective aerosol production fluxes while intensifying vertical transport, collectively lowering NCs. WS, SST, and SST-T_{2m} displayed distinct diurnal cycles,. whichThey may drive a distinct diurnal variation inof NCs. Compared with the daytime, the combination of lower WS and higher SST and SST-T_{2m} caused lower NCs at nighttime. During sunrise and sunset, rapid variations in meteorological parameters triggered NC fluctuations. In the NDT transition (the transition $period_1$), stable WS left SST and SST-T_{2m} as dominant NC regulators. In the DNT transition (the transition $period_2$), all aforementioned three factors jointly influenced NCs., with higher NCs in the daytime than in the nighttime. Meanwhile, during daytime-nighttime transition periods, the variations of NCs emerged as an apparent transition. At night, lower WS combined with higher SST and SST-T_{2m} minimized NCs. Rapid solar radiation shifts drove abrupt meteorological changes during sunrise and sunset, triggering NC fluctuations. In the NDT transition (the transition $period_1$), stable WS left SST and SST-T_{2m} as dominant NC regulators. In the DNT transition (the transition $period_2$), all the aforementioned three factors jointly influenced NCs.

Overall, this study filled data gaps and updated observational data for the SCS, while comprehensively analyzing diurnal variations in marine aerosols, impacts of continental transport, and potential influencing factors,Overall, this study gaps in and updated observational data for the SCS while comprehensively analyzing marine aerosol diurnal variations, continental transport impacts, and future investigated the potential factors, especially the SST-T_{2m} of theamong meteorological parameters. Theseis findings enables subsequent refinement of traditional marine aerosol sourcegeneration functions, which rely solely on WS and SST. However, the short-duration cruise data limited robust theoretical conclusions about SST and SST-T_{2m} effects on aerosols. Additionally, validating sea surface phenomena (e.g., whitecap coverage, an indicator of wave-driven aerosol production) against meteorological parameters remainsed challenging due to scarce on-site observations. Thus, more detailed observations and laboratory experiments will beere critical in future studies to validate the proposed influences of meteorological parameterselement influences and specific mechanisms underlyingon aerosol productiongeneration and transport.

Data Availability

All data from this research are available from the corresponding author upon request.

Author contributions

SC and TL designed this study. ZQ and HX performed the measurments during the cruise. MZ and YP implemented the back trajectory analysis. ZQ, XL, ZZ and SC analyzed the data. ZQ, SC and XW wrote the paper. All co-authors proofread and commented on the paper.

Competing interests

The authors declare that they have no known competing financial interests or personal relationships that could have appeared to influence the work reported in this paper.

Disclaimer

Publisher's note: Copernicus Publications remains neutral with regard to jurisdictional claims made in the text, published maps, institutional affiliations, or any other geographical representation in this paper. While Copernicus Publications makes every effort to include appropriate place names, the final responsibility lies with the authors.

Acknowledgments

The authors acknowledge the South China Sea Institute of Oceanology, the Chinese Academy of Sciences for supporting this research cruise. The authors thank Kun Zhang and Haoda Yang for helping install the instruments. The authors thank the Max-Planck Society for the provision of the PLC model used in this study. The authors thank the NOAA ARL for the provision of the HYSPLIT transport and dispersion model used in this study. The ERA5 hourly dataset used in this study was provided by the ECMWF, and the MERRA-2 dataset was provided by the GMAO at NASA Goddard Space Flight Center.

Financial support

This study was funded by the National 173 Basic Strengthening Program (No. XXX), Key Scientific Research Project of Anhui Education Department (No.2022AH051712), and Scientific Research Foundation for the Advanced Talents, Chaohu University (No. KYQD-202208).

References

Alexander, B., Park, R. J., Jacob, D. J., Li, Q. B., Yantosca, R. M., Savarino, J., Lee, C. C. W., and Thiemens, H.: Sulphate formation in sea-salt aerosols: Constraints from oxygen isotopes, J. Geophys. Res., 110, D1037, https://doi.org/10.1029/2004jd005659, 2005.

Andreas, E. L.: A new sea spray generation function for wind speeds up to 32 m s^{-1}, J. Phys. Oceanogr., 28, 2175–2184, https://doi.org/10.1175/1520-0485(1998)028<2175:ANSSGF>2.0.CO;2, 1998.

~~Andreas, E. L.: A review of spray generation function for the open ocean, in: Atmosphere–Ocean Interactions. edited by: Perrie, W. WTT Press, Billerica, Mass, 1–46, 2002.~~

Andreas, E. L.: Spray-mediated enthalpy flux to the atmosphere and salt flux to the ocean in high winds, J. Phys. Oceanogr., 40, 608–619, https://doi.org/10.1175/2009JPO4232.1., 2010.

Andreae, M. O., and Rosenfeld, D.: Aerosol-cloud-precipitation interactions. Part 1. The nature and sources of cloud-active aerosols, Earth-sci. Rev., 89, 13–41, https://doi.org/10.1016/j.earscirev.2008.03.001, 2008.

Andronache, C.: Estimated variability of below-cloud aerosol removal by rainfall for observed aerosol size distributions, Atmos. Chem. Phys., 3, 131–143, https://doi.org/10.5194/acp-3-131-2003, 2003.

Athanasopoulou, E., Protonotariou, A., Papangelis, G., Tombrou, M., and Gerasopoulos, E.: Long-range transport of Saharan dust and chemical transformations over the Eastern Mediterranean, Atmos. Environ., 140, 592–604, https://doi.org/10.1016/j.atmosenv.2016.06.041, 2016.

Atwood, S. A., Reid, J. S., Kreidenweis, S. M., Blake, D. R., Jonsson, H. H., Lagrosas, N. D., Xian, P., Reid, E. A., Sessions, W. R., and Simpas, J. B.: Size-resolved aerosol and cloud condensation nuclei (CCN) properties in the remote marine South China Sea – Part 1: Observations and source classification, Atmos. Chem. Phys., 17, 1105–1123, https://doi.org/10.5194/acp-17-1105-2017, 2017.

Arimoto, R., and Duce, R. A.: Dry deposition models and the air/sea exchange of trace elements, J. Geophys. Res., 91, 2787–2792, doi:10.1029/JD091iD02p02787, 1986.

Atlas, E. and Giam, C. S.: Ambient Concentration and Precipitation Scavenging of Atmospheric Organic Pollutants, Water Air Soil Poll., 38, 19–36, 1988.

Bauer, S. E., Tsigaridis, K., Faluvegi, G., Kelley, M., Lo, K. K., Miller, R. L., Nazarenko, L., Schmidt, G. A., and Wu, J. B.: Historical (1850–2014) aerosol evolution and role on climate forcing using the GISS ModelE2.1 contribution to CMIP6, J. Adv. Model Earth Sy., 12, e2019MS001978, https://doi.org/10.1029/2019MS001978, 2020.

Bird, J. C., de Ruiter, R., Courbin, L., and Stone, H. A.: Daughter bubble cascades produced by folding of ruptured thin films, Nature, 465,759-762, https://doi.org/10.1038/nature09069, 2010.

Blanchard, D. C., and Woodcock, A. H.: The production, concentration, and vertical distribution of the sea-salt aerosol, Ann. N. Y. Acad. Sci., 338, 330–347, https://doi.org/10.1111/j.1749-6632.1980.tb17130.x, 1980.

Braun, R. A., Aghdam, M. A., Bañaga, P. A., Betito, G., Cambaliza, M. O., Cruz, M. T., Lorenzo, G. R., MacDonald, A. B., Simpas, J. B., Stahl, C., and Sorooshian, A.: Long-range aerosol transport and impacts on size-resolved aerosol composition in Metro Manila, Philippines, Atmos. Chem. Phys., 20, 2387–2405, https://doi.org/10.5194/acp-20-2387-2020, 2020.

Bruch, W., Yohia, C., Tulet, P., Limoges, A., Sutherland, P., van Eijk, A. M. J., Missamou, T. and Piazzola, J.: Atmospheric sea spray modeling in the North-East Atlantic Ocean using tunnel-derived generation functions and the SUMOS cruise data set, J. Geophys. Res.-Atmos., 128, e2022JD038330, https://doi.org/10.1029/2022JD038330, 2023.

Bzdek, B. R., Reid, J. P., and Cotterell, M. I.: Open questions on the physical properties of aerosols, Comm. Chem., 3, 105, https://doi.org/10.1038/s42004-020-00342-9, 2020.

Cai, M., Liang, B. L., Sun, Q. B., Zhou, S. Z., Chen, X. Y., Yuan, B., Shao, M., Tan, H. B., and Zhao, J.: Effects of continental emissions on cloud condensation nuclei (CCN) activity in the northern South China Sea during summertime 2018, Atmos. Chem. Phys., 20, 9153–9167, https://doi.org/10.5194/acp-20-9153-2020, 2020.

Carslaw, K. S., Boucher, O., Spracklen, D. V., Mann, G. W., Rae, J. G. L., Woodward, S., and Kulmala, M.: A review of natural aerosol interactions and feedbacks within the Earth system, Atmos. Chem. Phys., 10, 1701–1737, https://doi.org/10.5194/acp-10-1701-2010, 2010.

Chen, S. P., Lu, C. H., Queen, J. M., and Lee, P.: Application of satellite observations in conjunction with aerosol reanalysis to characterize long-range transportof African and Asian dust on air quality in the contiguous U.S, Atmos. Environ., 187, 174–195, https://doi.org/10.1016/j.atmosenv.2018.05.038, 2018.

Christiansen, S., Salter, M. E., Gorokhova, E., Nguyen, Q. T., and Bilde, M.: Sea spray aerosol formation: Laboratory results on the role of air entrainment, water temperature, and phytoplankton biomass, Environ. Sci. Technol., 53, 13107–13116, https://doi.org/10.1021/acs.est.9b04078, 2019.

Dasarathy, S., Russell, L. M., Rodier, S. D., and Bowman, J. S.: Wind-Driven and Seasonal Effects on Marine Aerosol Production in the Bellingshausen Sea, Antarctica, Geophys. Res. Lett., 50, e2022GL099723. https://doi.org/10.1029/2022GL099723, 2023.

Decesari, S., Finessi, E., Rinaldi, M., Paglione, M., Fuzzi, S., Stephanou, E. G., Tziaras, T., Spyros, A., Ceburnis, D., O'Dowd, C., Dall'Osto, M., Harrison, R. M., Allan, J., Coe, H., and Facchini, M. C.: Primary and secondary marine aerosols over the North Atlantic Ocean during the MAP experiment, J. Geophys. Res., 116, 1–21, https://doi.org/10.1029/2011JD016204, 2011.

Dedrick, J. L., Saliba, G., Williams, A. S., Russell, L. M., and Lubin, D.: Retrieval of the sea spray aerosol mode from submicron particle size distributions and supermicron scattering during LASIC, Atmos. Meas. Tech., 15, 4171–4194, https://doi.org/10.5194/amt-15-4171-2022, 2022.

Ding, J., Dai, Q., Zhang, Y., Xu, J., Huangfu, Y., and Feng, Y.: Air humidity affects secondary aerosol formation in different pathways, Sci. Total Environ., 759, 143540, https://doi.org/10.1016/j.scitotenv.2020.143540, 2021.

Duce, R. A., Winchester, J. W., and Van Nahl, T. W.: Iodine, bromine, and chlorine in the Hawaiian marine atmosphere, J. Geophys. Res., 70, 1775–1799, https://doi.org/10.1029/JZ070i008p01775, 1965.

~~Ehn, M., Vuollekoski, H., Petäjä, T., Kerminen, V.-M., Vana, M., Aalto, P., de Leeuw, G., Ceburnis, D., Dupuy, R., O'Dowd, C. D., and Kulmala, M.: Growth rates during coastal and marine new particle formation in western Ireland, J. Geophys. Res.-Atmos., 115, https://doi.org/10.1029/2010JD014292, 2010.~~

Eriksson, E.: The yearly circulation of chloride and sulfur in nature: Meteorological, geochemical and pedological implications. Part II, Tellus, 11, 375-403, https://doi.org/10.1111/j.2153-3490.1960.tb01284.x, 1960.

Feingold, G., Cotton, W. R., Kreidenweis, S. M., and Davis, J. T.: The Impact of Giant Cloud Condensation Nuclei on Drizzle Formation in Stratocumulus: Implications for Cloud Radiative Properties, J. Atmos. Sci., 56, 4100-4117, https://doi.org/10.1175/1520-0469(1999)056<4100:TIOGCC>2.0.CO;2, 1999.

Flores, J. M., Bourdin, G., Altaratz, O., Trainic, M., Lang-Yona, N., Dzimban, E., Steinau, S., Tettich, F., Planes, S., Allemand, D., Agostini, S., Banaigs, B., Boissin, E., Boss, E., Douville, E., Forcioli, D., Furla, P., Galand, P. E., Sullivan, M. B., Gilson, É., Lombard, F., Moulin, C., Pesant, S., Poulain, J., Reynaud, S., Romac, S., Sunagawa, S., Thomas, O. P., Troublé, R., de Vargas, C., Thurber, R. V., Voolstra, C. R., Wincker, P., Zoccola, D., Bowler, C., Gorsky, G., Rudich, Y., Vardi, A., and Koren, I.: Tara Pacific Expedition's Atmospheric Measurements of Marine Aerosols across the Atlantic and Pacific Oceans: Overview and Preliminary Results, Bull. Am. Meteorol. Soc., 101, E536-E554, https://doi.org/10.1175/BAMS-D-18-0224.1, 2020.

Flores, J. M., Bourdin, G., Kostinski, A. B., Altaratz, O., Dagan, G., Lombard, F., Haëntjens, N., Boss, E., Sullivan, M. B., Gorsky, G., Lang-Yona, N., Trainic, M., Romac, S., Voolstra, C. R., Rudich, Y., Vardi, A., and Koren, I.: Diel cycle of sea spray aerosol concentration, Nat. Commun., 12, 5476, https://doi.org/10.1038/s41467-021-25579-3, 2021.

Forestieri, S. D., Moore, K. A., Martinez Borrero, R., Wang, A., Stokes, M. D., and Cappa, C. D.: Temperature and Composition Dependence of Sea Spray Aerosol Production, Geophys. Res. Lett., 45, 7218-7225, https://doi.org/10.1029/2018GL078193, 2018.

Gathman, S. G.: Optical Properties Of The Marine Aerosol As Predicted By The Navy Aerosol Model, Opt. Eng., 22, 220157, 1983.

Gelaro, R., McCarty, W., Suárez, M. J., Todling, R., Molod, A., Takacs, L., Randles, C. A., Darmenov, A., Bosilovich, M. G., Reichle, R., Wargan, K., Coy, L., Cullather, R., Draper, C., Akella, S., Buchard, V., Conaty, A., Silva, A. M. da, Gu, W., Kim, G.-K., Koster, R., Lucchesi, R., Merkova, D., Nielsen, J. E., Partyka, G., Pawson, S., Putman, W., Rienecker, M., Schubert, S. D., Sienkiewicz, M., and Zhao, B.: The Modern-Era Retrospective Analysis for Research and Applications, Version 2 (MERRA-2), J. Climate, 30, 5419–5454, https://doi.org/10.1175/jcli-d-16-0758.1, 2017.

Geng, X., Haig, J., Lin, B., Tian, C., Zhu, S., Cheng, Z., Yuan, Y., Zhang, Y., Liu, J., Zheng, M., Li, J., Zhong, G., Zhao, S., Bird, M. I., Zhang, G.: Provenance of Aerosol Black Carbon over Northeast Indian Ocean and South China

Sea and Implications for Oceanic Black Carbon Cycling, Environ. Sci. Technol., 57, 13067-13078, https://doi.org/10.1021/acs.est.3c03481, 2023.

Global Modeling and Assimilation Office (GMAO): MERRA-2 tavg1_2d_aer_Nx: 2d,1-Hourly,Time-averaged,Single-Level,Assimilation,Aerosol Diagnostics V5.12.4, Greenbelt, MD, USA, Goddard Earth Sciences Data and Information Services Center (GES DISC) [data set], https://doi.org/10.5067/7MCPBJ41Y0K6, 2015.

Gong, S. L.: A parameterization of sea-salt aerosol source function for sub- and super-micron particles, Global Biogeochem. Cy., 17, 1097, https://doi.org/10.1029/2003gb002079, 2003.

Croft, B., Martin, R. V., Moore, R. H., Ziemba, L. D., Crosbie, E. C., Liu, H., Russell, L. M., Saliba, G., Wisthaler, A., Müller, M., Schiller, A., Galí, M., Chang, R. Y.-W., McDuffie, E. E., Bilsback, K. R., and Pierce, J. R.: Factors controlling marine aerosol size distributions and their climate effects over the northwest Atlantic Ocean region, Atmos. Chem. Phys., 21, 1889–1916, https://doi.org/10.5194/acp-21-1889-2021, 2021.

Han, S., Cai, Z., Liu, J., Zhang, M., Chen, J., and Lin, Y.: Comparison on aerosol physicochemical properties of sea and land along the coast of Bohai, China, Sci. Total Environ., 673, 148-156, https://doi.org/10.1016/j.scitotenv.2019.04.040, 2019.

Hersbach, H., Bell, B., Berrisford, P., Biavati, G., Horányi, A., Muñoz Sabater, J., Nicolas, J., Peubey, C., Radu, R., Rozum, I., Schepers, D., Simmons, A., Soci, C., Dee, D., and Thépaut, J.-N.: ERA5 monthly averaged data on single levels from 1940 to present, https://doi.org/10.24381/cds.f17050d7, 2023.

Hodshire, A. L., Akherati, A., Alvarado, M. J., Brown-Steiner, B., Jathar, S. H., Jimenez, J. L., Kreidenweis, S. M., Lonsdale, C. R., Onasch, T. B., Ortega, A. M., and Pierce, J. R.: Aging Effects on Biomass Burning Aerosol Mass and Composition: A Critical Review of Field and Laboratory Studies, Environ. Sci. Technol., 53, 10007–10022, https://doi.org/10.1021/acs.est.9b02588, 2019.

Hoppel, W. A.: Measurement of the Size Distribution and CCN Supersaturation Spectrum of Submicron Aerosols over the Ocean, J. Atmos. Sci., 36, 2006-2015, https://doi.org/10.1175/1520-0469(1979)036<2006:MOTSDA>2.0.CO;2, 1979.

Hoppel, W. A., Fitzgerald, J. W., and Larson, R. E.: Aerosol size distributions in air masses advecting off the east coast of the United States, J. Geophys. Res.-Atmos., 90, 2365-2379, https://doi.org/10.1029/JD090iD01p02365, 1985.

Irshad, R., Grainger, R. G., Peters, D. M., McPheat, R. A., Smith, K. M., and Thomas, G.: Laboratory measurements of the optical properties of sea salt aerosol, Atmos. Chem. Phys., 9, 221-230, https://doi.org/10.5194/acp-9-221-2009, 2009.

Jaeglé, L., Quinn, P. K., Bates, T. S., Alexander, B., and Lin, J. T.: Global distribution of sea salt aerosols: new constraints from in situ and remote sensing observations, Atmos. Chem. Phys., 11, 3137-3157, https://doi.org/10.5194/acp-11-3137-2011, 2011.

Jiang, B., Xie, Z., Lam, P. K. S., He, P., Yue, F., Wang, L., Huang, Y., Kang, H., Yu, X., and Wu, X.: Spatial and temporal distribution of sea salt aerosol mass concentrations in the marine boundary layer from the Arctic to the Antarctic, J. Geophys. Res.-Atmos., 126, e2020JD033892, https://doi.org/10.1029/2020JD033892, 2021.

Jing, Z., Chang, P., Shan, X., Wang, S., Wu, L., and Kurian, J.: Mesoscale SST dynamics in the Kuroshio–Oyashio extension region, J. Phys. Oceanogr., 49, 1339-1352, https://doi.org/10.1175/JPO-D-18-0159.1, 2019.

Joung, Y., Buie, C.: Aerosol generation by raindrop impact on soil, Nat. Commun., 6, 6083, https://doi.org/10.1038/ncomms7083, 2015.

Keene, W. C., Long, M. S., Reid, J. S., Frossard, A. A., Kieber, D. J., Maben, J. R., Russell, L. M., Kinsey, J. D., Quinn, P. K., and Bates, T. S.: Factors that modulate properties of primary marine aerosol generated from ambient seawater on ships at sea, J. Geophys. Res.-Atmos., 122, 11,961-911,990, https://doi.org/10.1002/2017JD026872, 2017.

Kettle, A. J. and Andreae, M. O.: Flux of dimethylsulfide from the oceans: A comparison of updated data sets and flux models, J. Geophys. Res., 105, 26793–26808, https://doi.org/10.1029/2000JD900252, 2000.

Kim, J. H., Yum, S. S., Lee, Y. G., and Choi, B. C.: Ship measurements of submicron aerosol size distributions over the Yellow Sea and the East China Sea, Atmos. Res., 93, 700-714, https://doi.org/10.1016/j.atmosres.2009.02.011, 2009.

Kong, Y. W., Sheng, L. F., Liu, Q., and Li, X. Z.: Impact of marine atmospheric process on aerosol number size distribution in the South China Sea, (in Chinese), Environ. Sci., 37, 2443-2452, 10.13227/j.hjkx.2016.07.005, 2016.

Korhonen, H., Carslaw, K. S., Spracklen, D. V., Mann, G. W., and Woodhouse, M. T.: Influence of oceanic dimethyl sulfide emissions on cloud condensation nuclei concentrations and seasonality over the remote Southern Hemisphere oceans: a global model study, J. Geophys. Res.-Atmos., 113, 1–16, https://doi.org/10.1029/2007JD009718, 2008.

~~Kuang, C., McMurry, P. H., and McCormick, A. V.: Determination of cloud condensation nuclei production from measured new particle formation events, Geophys. Res. Lett., 36, https://doi.org/10.1029/2009GL037584, 2009.~~

Lawler, M. J., Sander, R., Carpenter, L. J., Lee, J. D., von Glasow, R., Sommariva, R., and Saltzman, E. S.: HOCl and Cl2 observations in marine air, Atmos. Chem. Phys., 11, 7617-7628, 10.5194/acp-11-7617-2011, 2011.

Leck, C. and Persson, C.: Seasonal and short-term variability in dimethyl sulfide, sulfur dioxide and biogenic sulfur and sea salt aerosol particles in the arctic marine boundary layer during summer and autumn, Tellus B, 48, 272–299, https://doi.org/10.3402/tellusb.v48i2.15891, 1996.

Levin, Z., Teller, A., Ganor, E., and Yin, Y.: On the interactions of mineral dust, sea-salt particles, and clouds: A measurement and modeling study from the Mediterranean Israeli Dust Experiment campaign, J. Geophys. Res.-Atmos., 110, D20202, https://doi.org/10.1029/2005JD005810, 2005.

Lewis, E. and Schwartz, S.: Sea Salt Aerosol Production: Mechanisms, Methods, Measurements and Models—A Critical Review, Washington DC American Geophysical Union Geophysical Monograph Series, 152, 3719, 10.1029/GM152, 2004.

Li, J., Carlson, B. E., Yung, Y. L., Lv, D., Hansen, J., Penner, J. E., Liao, H., Ramaswamy, V., Kahn, R. A., Zhang, P., Dubovik, O., Ding, A., Lacis, A. A., Zhang, L., and Dong, Y.: Scattering and absorbing aerosols in the climate system, Nat. Rev. Earth Environ., 3, 363-379, 10.1038/s43017-022-00296-7, 2022.

Li, M., Zhang, Q., Kurokawa, J. I., Woo, J. H., He, K., Lu, Z., Ohara, T., Song, Y., Streets, D. G., Carmichael, G. R., Cheng, Y., Hong, C., Huo, H., Jiang, X., Kang, S., Liu, F., Su, H., and Zheng, B.: MIX: a mosaic Asian anthropogenic

emission inventory under the international collaboration framework of the MICS-Asia and HTAP, Atmos. Chem. Phys., 17, 935–963, https://doi.org/10.5194/acp-17-935-2017, 2017.

Liang, B., Cai, M., Sun, Q., Zhou, S., and Zhao, J.: Source apportionment of marine atmospheric aerosols in northern South China Sea during summertime 2018, Environ. Pollut., 289, 117948, https://doi.org/10.1016/j.envpol.2021.117948, 2021.

Lin, P., Hu, M., Wu, Z., Niu, Y., and Zhu, T.: Marine aerosol size distributions in the springtime over China adjacent seas, Atmos. Environ., 41, 6784-6796, https://doi.org/10.1016/j.atmosenv.2007.04.045, 2007.

Lo, A. K., Zhang, L., Sievering, H.: The effect of humidity and state of water surfaces on deposition of aerosol particles onto a water surface, Atmos. Environ., 33, 4727–4737, https://doi.org/10.1016/S1352-2310(99)00202-2, 1999.

Long, M. S., Keene, W. C., Easter, R. C., Sander, R., Liu, X., Kerkweg, A., and Erickson, D.: Sensitivity of tropospheric chemical composition to halogen-radical chemistry using a fully coupled size-resolved multiphase chemistry–global climate system: halogen distributions, aerosol composition, and sensitivity of climate-relevant gases, Atmos. Chem. Phys., 14, 3397-3425, https://doi.org/10.5194/acp-14-3397-2014, 2014.

Lorenzo, G. R., Arellano, A. F., Cambaliza, M. O., Castro, C., Cruz, M. T., Di Girolamo, L., Gacal, G. F., Hilario, M. R. A., Lagrosas, N., Ong, H. J., Simpas, J. B., Uy, S. N., and Sorooshian, A.: An emerging aerosol climatology via remote sensing over Metro Manila, the Philippines, Atmos. Chem. Phys., 23, 10579–10608, https://doi.org/10.5194/acp-23-10579-2023, 2023.

Ma, X., Jing, Z., Chang, P., Liu, X., Montuoro, R., Small, R. J., Bryan, F. O., Greatbatch, R. J., Brandt, P., Wu, D., Lin, X., and Wu, L.: Western boundary currents regulated by interaction between ocean eddies and the atmosphere, Nature, 535, 533-537, https://doi.org/10.1038/nature18640, 2016.

Ma, Y., Zhang, X., Xin, J., Zhang, W., Wang, Z., Liu, Q., Wu, F., Wang, L., Lyu, Y., Wang, Q., and Ma, Y.: Mass and number concentration distribution of marine aerosol in the Western Pacific and the influence of continental transport, Environ. Pollut., 298, 118827, https://doi.org/10.1016/j.envpol.2022.118827, 2022.

Mårtensson, E. M., Nilsson, E. D., de Leeuw, G., Cohen, L. H., and Hansson, H.-C.: Laboratory simulations and parameterization of the primary marine aerosol production, J. Geophys. Res.-Atmos., 108, 4297, https://doi.org/10.1029/2002JD002263, 2003.

Meinrat, O.Andreae., and Paul, J.Crutzen.: Atmospheric Aerosols: Biogeochemical Sources and Role in Atmospheric Chemistry, Science, 276, 1052-1058, DOI: 10.1126/science.276.5315.1052, 1997.

Miguet, J., Rouyer, F., and Rio, E.: The Life of a Surface Bubble, Molecules, 26, 1317, https://doi.org/10.3390/molecules26051317, 2021.

Myhre, G., Stordal, F., Johnsrud, M., Ignatov, A., Mishchenko, M. I., Geogdzhayev, I. V., Tanré, D., Deuzé, J.-L., Goloub, P., Nakajima, T., Higurashi, A., Torres, O., and Holben, B.: Intercomparison of Satellite Retrieved Aerosol Optical Depth over the Ocean, J. Atmos. Sci., 61, 499-513, https://doi.org/10.1175/1520-0469(2004)061<0499:IOSRAO>2.0.CO;2, 2004.

Nascimento, J. P., Bela, M. M., Meller, B. B., Banducci, A. L., Rizzo, L. V., Vara-Vela, A. L., Barbosa, H. M. J., Gomes, H., Rafee, S. A. A., Franco, M. A., Carbone, S., Cirino, G. G., Souza, R. A. F., McKeen, S. A., and Artaxo, P.: Aerosols from anthropogenic and biogenic sources and their interactions – modeling aerosol formation, optical properties, and impacts over the central Amazon basin, Atmos. Chem. Phys., 21, 6755–6779, https://doi.org/10.5194/acp-21-6755-2021, 2021.

Nguyen, Q. T., Kjær, K. H., Kling, K. I., Boesen, T., and Bilde, M.: Impact of fatty acid coating on the CCN activity of sea salt particles, Tellus B, 69, 1–15, 1304064, https://doi.org/10.1080/16000889.2017.1304064, 2017.

O'Dowd, C. D. and de Leeuw, G.: Marine aerosol production: a review of the current knowledge, Philos. T. R. Soc. A, 365, 1753-1774, https://doi.org/10.1098/rsta.2007.2043, 2007.

O'Dowd, C. D., Jimenez, J. L., Bahreini, R., Flagan, R. C., Seinfeld, J. H., Hämeri, K., Pirjola, L., Kulmala, M., Jennings, S. G., and Hoffmann, T.: Marine aerosol formation from biogenic iodine emissions, Nature, 417, 632, https://doi.org/10.1038/nature00775, 2002.

Ohata, S., Moteki, N., Mori, T., Koike, M., and Kondo, Y.: A key process controlling the wet removal of aerosols: new observational evidence, Sci. Rep.-UK, 6, 34113, https://doi.org/10.1038/srep34113, 2016.

O'Neill, L. W., Chelton, D. B., and Esbensen, S. K.: The effects of SST-induced surface wind speed and direction gradients on midlatitude surface vorticity and divergence, J. Climate, 23, 255-281, https://doi.org/10.1175/2009JCLI2613.1, 2010.

Ovadnevaite, J., Manders, A., de Leeuw, G., Ceburnis, D., Monahan, C., Partanen, A. I., Korhonen, H., and O'Dowd, C. D.: A sea spray aerosol flux parameterization encapsulating wave state, Atmos. Chem. Phys., 14, https://doi.org/10.5194/acp-14-1837-2014, 2014.

Pagels, J., Gudmundsson, A., Gustavsson, E., Asking, L., and Bohgard, M.: Evaluation of aerodynamic particle sizer and electrical low-pressure impactor for unimodal and bimodal mass-weighted size distributions, Aerosol Sci. Tech., 39, 871-887, 2005.

Pant, V., Deshpande, C. G., and Kamra, A. K.: The concentration and number size distribution measurements of the Marine Boundary Layer aerosols over the Indian Ocean, Atmos. Res., 92, 381-393, https://doi.org/10.1016/j.atmosres.2008.12.004, 2009.

Peters, T. M., and Leith D.: Concentration measurement and counting efficiency of the aerodynamic particle sizer 3321, J. Aerosol Sci., 34, 627-634, 2003.

Peters, T. M.: Use of the Aerodynamic Particle Sizer to measure ambient $PM_{10-2.5}$: The coarse fraction of PM_{10}, J. Air Waste Manage., 56, 411-416, 2006.

Pfeifer, S., Müller, T., Weinhold, K., Zikova, N., Martins dos Santos, S., Marinoni, A., Bischof, O. F., Kykal, C., Ries, L., Meinhardt, F., Aalto, P., Mihalopoulos, N., and Wiedensohler, A.: Intercomparison of 15 aerodynamic particle size

spectrometers (APS 3321): uncertainties in particle sizing and number size distribution, Atmos. Meas. Tech., 9, 1545–1551, https://doi.org/10.5194/amt-9-1545-2016, 2016.

Prospero, J.M.: Mineral and sea salt aerosol concentrations in various ocean regions, J. Geophys. Res.-Oceans, 84, 725–731, https://doi.org/10.1029/JC084iC02p00725, 1979.

Provençal, S., Buchard, V., da Silva, A. M., Leduc, R., and Barrette, N.: Evaluation of PM surface concentrations simulated by Version 1 of NASA's MERRA Aerosol Reanalysis over Europe, Atmos. Pollut. Res., 8, 374-382, https://doi.org/10.1016/j.apr.2016.10.009, 2017a.

Provençal, S., Buchard, V., Silva, A. M. d., Leduc, R., Barrette, N., Elhacham, E., and Wang, S. H.: Evaluation of PM2.5 Surface Concentrations Simulated by Version 1 of NASA's MERRA Aerosol Reanalysis over Israel and Taiwan, Aerosol Air Qual. Res., 17, 253-261, https://doi.org/10.4209/aaqr.2016.04.0145, 2017b.

Radke, L. F., Hobbs, P. V., and Eltgroth, M. W.: Scavenging of Aerosol Particles by Precipitation, J. Appl. Meteorol., 19, 715–722, 1980.

Randles, C. A., Da Silva, A. M., Buchard, V., Colarco, P. R., Darmenov, A., Govindaraju, R., Smirnov, A., Holben, B., Ferrare, R., Hair, J., and Shinozuka, Y.: The MERRA-2 aerosol reanalysis 1980 onward. Part I, System description and data assimilation evaluation, J. Climate, 30, 6823-6850, 2017.

Russell, L. M., Huebert, B. J., Flagan, R. C., and Seinfeld, J. H.: Characterization of submicron aerosol size distributions from time-resolved measurements in the Atlantic Stratocumulus Transition Experiment Marine Aerosol and Gas Exchange, J. Geophys. Res.-Atmos., 101, 4469–4478, https://doi.org/10.1029/95JD01372, 1996.

Saha, S., Sharma, S., Chhabra, A., Kumar, K. N., Kumar., P., Kamat, D., Lal, S..: Impact of dust storm on the atmospheric boundary layer: a case study from western India, Nat. Hazards, 113, 143–155, https://doi.org/10.1007/s11069-022-05293-z, 2022.

Sakerin, S. M., Bobrikov, A. A., Bukin, O. A., Golobokova, L. P., Pol'kin, Vas. V., Pol'kin, Vik. V., Shmirko, K. A., Kabanov, D. M., Khodzher, T. V., Onischuk, N. A., Pavlov, A. N., Potemkin, V. L., and Radionov, V. F.: On measurements of aerosol-gas composition of the atmosphere during two expeditions in 2013 along the Northern Sea Route, Atmos. Chem. Phys., 15, 12413–12443, https://doi.org/10.5194/acp-15-12413-2015, 2015.

Saliba, G., Chen, C.-L., Lewis, S., Russell, L. M., Rivellini, L.-H., Lee, A. K. Y., Quinn, P. K., Bates, T. S., Haëntjens, N., Boss, E. S., Karp-Boss, L., Baetge, N., Carlson, C. A., and Behrenfeld, M. J.: Factors driving the seasonal and hourly variability of sea-spray aerosol number in the North Atlantic, P. Natl. Acad. Sci. USA., 116, 20309-20314, https://doi.org/10.1073/pnas.1907574116, 2019.

Saliba, G., Chen, C., Lewis, S., Russell, L. M., Quinn, P. K., Bates, T. S., Bell, T. G., Lawler, M. J., Saltzman, E. S., Sanchez, K. J., Moore, R., Shook, M., Rivellini, L., Lee, A., Baetge, N., Carlson, C. A., and Behrenfeld, M. J.: Seasonal Differences and Variability of Concentrations, Chemical Composition, and Cloud Condensation Nuclei of Marine Aerosol Over the North Atlantic, J. Geophys. Res.-Atmos., 125, e2020JD033145, https://doi.org/10.1029/2020JD033145, 2020.

Salter, M. E., Nilsson, E. D., Butcher, A., and Bilde, M.: On the seawater temperature dependence of the sea spray aerosol generated by a continuous plunging jet, J. Geophys. Res.-Atmos., 119, 9052-9072, https://doi.org/10.1002/2013JD021376, 2014.

Sander, R., Keene, W. C., Pszenny, A. A. P., Arimoto, R., Ayers, G. P., Baboukas, E., Cainey, J. M., Crutzen, P. J., Duce, R. A., Hönninger, G., Huebert, B. J., Maenhaut, W., Mihalopoulos, N., Turekian, V. C., and Van Dingenen, R.: Inorganic bromine in the marine boundary layer: a critical review, Atmos. Chem. Phys., 3, 1301-1336, https://doi.org/10.5194/acp-3-1301-2003, 2003.

Savoie, D. L., Prospero, J. M., Larsen, R. J., Huang, F., Izaguirre, M. A., Huang, T., Snowdon, T. H., Custals, L., and Sanderson, C. G.: Nitrogen and sulfur species in Antarctic aerosols at Mawson, Palmer Station, and Marsh (King George Island), J. Atmos. Chem., 17, 95-122, https://doi.org/10.1007/bf00702821, 1993.

Sellegri, K., O'Dowd, C. D., Yoon, Y. J., Jennings, S. G., and de Leeuw, G.: Surfactants and submicron sea spray generation, J. Geophys. Res.-Atmos., 111, D22215, https://doi.org/10.1029/2005JD006658, 2006.

Sellegri, K., Barthelmeß, T., Trueblood, J., Cristi, A., Freney, E., Rose, C., Barr, N., Harvey, M., Safi, K., Deppeler, S., Thompson, K., Dillon, W., Engel, A., and Law, C.: Quantified effect of seawater biogeochemistry on the temperature dependence of sea spray aerosol fluxes, Atmos. Chem. Phys., 23, 12949-12964, https://doi.org/10.5194/acp-23-12949-2023, 2023.

Smith, M. H., Park, P. M., and Consterdine, I. E.: Marine aerosol concentrations and estimated fluxes over the sea, Q. J. Rol. Meteor. Soc., 119, 809-824, https://doi.org/10.1002/qj.49711951211, 1993.

Solomon, S., Daniel, J. S., Neely, III, R. R., Vernier, J.-P., Dutton, E. G., and Thomason, L. W.: The Persistently Variable "Background" Stratospheric Aerosol Layer and Global Climate Change, Science, 333, 866-870, DOI:10.1126/science.1206027, 2011.

Song, A., Li, J., Tsona, N. T., and Du, L.: Parameterizations for sea spray aerosol production flux, Appl. Geochem., 157, 105776, https://doi.org/10.1016/j.apgeochem.2023.105776, 2023.

Su, Y., Han, Y., Luo, H., Zhang, Y., Shao, S., and Xie, X.: Physical-optical properties of marine aerosols over the South China Sea: shipboard measurements and MERRA-2 reanalysis, Remote Sens., 14, 2453, https://doi.org/10.3390/rs14102453, 2022.

~~Tang, I. N.: Thermodynamic and optical properties of sea salt aerosol, J. Geophys. Res., 102, 23269-23275, https://doi.org/10.1029/97JD01806, 1997~~

Textor, C., Schulz, M., Guibert, S., Kinne, S., Balkanski, Y., Bauer, S., Berntsen, T., Berglen, T., Boucher, O., Chin, M., Dentener, F., Diehl, T., Easter, R., Feichter, H., Fillmore, D., Ghan, S., Ginoux, P., Gong, S., Grini, A., Hendricks, J., Horowitz, L., Huang, P., Isaksen, I., Iversen, I., Kloster, S., Koch, D., Kirkevåg, A., Kristjansson, J. E., Krol, M., Lauer, A., Lamarque, J. F., Liu, X., Montanaro, V., Myhre, G., Penner, J., Pitari, G., Reddy, S., Seland, Ø., Stier, P., Takemura, T., and Tie, X.: Analysis and quantification of the diversities of aerosol life cycles within AeroCom, Atmos. Chem. Phys., 6, 1777-1813, https://doi.org/10.5194/acp-6-1777-2006, 2006.

Troitskaya, Y., Kandaurov, A., Ermakova, O., Kozlov, D., Sergeev, D., and Zilitinkevich, S.: The "bag breakup" spume droplet generation mechanism at high winds. Part I: Spray generation functionr, J. Phys. Oceanogr., 48, 2167–2188, https://doi.org/10.1175/jpo-d-17-0104.1, 2018.

VanCuren, R. A.: Asian aerosols in North America: Extracting the chemical composition and mass concentration of the Asian continental aerosol plume from long-term aerosol records in the western United States, J. Geophys. Res., 108, 4623, https://doi.org/10.1029/2003JD003459, 2003.

von der Weiden, S.-L., Drewnick, F., and Borrmann, S.: Particle Loss Calculator – a new software tool for the assessment of the performance of aerosol inlet systems, Atmos. Meas. Tech., 2, 479–494, https://doi.org/10.5194/amt-2-479-2009, 2009.

Wang, Y., Zheng, X., Dong, X., Xi, B., Wu, P., Logan, T., and Yung, Y. L.: Impacts of long-range transport of aerosols on marine-boundary-layer clouds in the eastern North Atlantic, Atmos. Chem. Phys., 20, 14741 – 14755, https://doi.org/10.5194/acp-20-14741-2020, 2020.

~~Wise, M. E., Freney, E. J., Tyree, C. A., Allen, J. O., Martin, S. T., Russell, L. M., and Buseck, P. R.: Hygroscopic behavior and liquid-layer composition of aerosol particles generated from natural and artificial seawater, J. Geophys. Res.-Atmos., 114, D03201, https://doi.org/10.1029/2008JD010449, 2009.~~

Woodcock, A. H.: Atmospheric seasalt particles and raindrops, J. Atmos. Sci., 9, 200-212, https://doi.org/10.1175/1520-0469(1952)009<0200:ASPAR>2.0.CO;2, 1952.

Woodcock, A. H.: Salt nuclei in marine air as a function of altitude and wind force, J. Atmos. Sci., 10, 362-371, https://doi.org/10.1175/1520-0469(1953)010<0366:SNIMAA>2.0.CO;2, 1953.

Woods, E., Chung, D., Lanney, H. M., and Ashwell, B. A.: Surface morphology and phase transitions in mixed Nacl/MgSO4 aerosol particles, J. Phys. Chem. A, 114, 2837-2844, https://doi.org/10.1021/jp911133j, 2010.

Wu, T. and Boor, B. E.: Urban aerosol size distributions: a global perspective, Atmos. Chem. Phys., 21, 8883–8914, https://doi.org/10.5194/acp-21-8883-2021, 2021.

Xu, L., Liu, X., Gao, H., Yao, X., Zhang, D., Bi, L., Liu, L., Zhang, J., Zhang, Y., Wang, Y., Yuan, Q., and Li, W.: Long-range transport of anthropogenic air pollutants into the marine air: insight into fine particle transport and chloride depletion on sea salts, Atmos. Chem. Phys., 21, 17715–17726, https://doi.org/10.5194/acp-21-17715-2021, 2021.

Yan, J., Lin, Q., Zhang, M. M., Zhao, S. H., and Chen, L. Q.: Effect of air masses motion on the rapid change of aerosols in marine atmosphere, J. Environ. Sci., 83, 217-228, https://doi.org/10.1016/j.jes.2019.04.005, 2019.

Yang, M., Norris, S. J., Bell, T. G., and Brooks, I. M.: Sea spray fluxes from the southwest coast of the United Kingdom–dependence on wind speed and wave height, Atmos. Chem. Phys., 19, 15271-15284, https://doi.org/10.5194/acp-19-15271-2019, 2019.

Yuan, R., Zhang, X., Liu, H., Gui, Y., Shao, B., Tao, X., Wang, Y., Zhong, J., Li, Y., and Gao, Z.: Aerosol vertical mass flux measurements during heavy aerosol pollution episodes at a rural site and an urban site in the Beijing area of the North China Plain, Atmos. Chem. Phys., 19, 12857-12874, https://doi.org/10.5194/acp-19-12857-2019, 2019.

Zábori, J., Matisāns, M., Krejci, R., Nilsson, E. D., and Ström, J.: Artificial primary marine aerosol production: a laboratory study with varying water temperature, salinity, and succinic acid concentration, Atmos. Chem. Phys., 12, 10709-10724, https://doi.org/10.5194/acp-12-10709-2012, 2012a.

Zábori, J., Krejci, R., Ekman, A. M. L., Mårtensson, E. M., Ström, J., de Leeuw, G., and Nilsson, E. D.: Wintertime Arctic Ocean sea water properties and primary marine aerosol concentrations, Atmos. Chem. Phys., 12, 10405-10421, https://doi.org/10.5194/acp-12-10405-2012, 2012b.

~~Zeng, J., Zhang, G., Long, S., Liu, K., Cao, L., Bao, L., and Li, Y.: Sea salt deliquescence and crystallization in atmosphere: an in situ investigation using x-ray phase contrast imaging, Surf. Interface Anal., 45, 930-936, https://doi.org/10.1002/sia.5184, 2013.~~

Zhou, K., Wang, S., Lu, X., Chen, H., Wang, L., Chen, J., Yang, X., Wang, X.: Production flux and chemical characteristics of spray aerosol generated from raindrop impact on seawater and soil, J. Geophys. Res.-Atmos., 125, e2019JD032052, https://doi.org/ 10.1029/2019JD032052, 2020.

Figure captions

~~Fig. 1 The calculated particle losses for the Model 3321 APS spectrometer in this cruise.~~

Fig. ~~2~~1 The total view of (a) the Model 3321 APS spectrometer and (b) the automatic meteorological observation system.

Fig. ~~3~~2 The time series of the observations on 25 May 2023. The black circle represented one case of ship pollution. (a) Trends of the aerosol size distributions. (b) Trends of the rainfall intensity and the WD.

Fig. ~~4~~3 The time series of the shipboard observations in the SCS from 21 May to 3 June 2023. The blue-shaded regions represented periods affected by rain events. (a) Trend of the aerosol size distributions. (b) Trends of NCs of the two aerosol particle modes (black solid line represented the NC of the coarse mode, and red solid line represented the NC of the accumulation mode). (c) Trend of the WD. (d) Trends of the T_{OBS} (dark orange solid line), T_{2m} (light orange solid line), and SST (blue solid line). (e) Trends in the RH (gray solid line), the VIS (red solid line), and the rainfall intensity (dark blue solid line).

Fig. ~~5~~4 (a) NC of the aerosol accumulation mode, (b) NC of the aerosol coarse mode, (c) RH, and (d) rainfall intensity as the functions of the WS and WD for the observations in the SCS.

Fig. 5 The scatter plots of (a) NCs of the aerosol accumulation mode and WS, (b) NCs of the aerosol coarse mode and WS. The observational data were binned to the WS intervals equal to 3 m s^{-1}; the boxes represented the 25th to 75th percentile value, the black whisker represented the 1.5 inter-quartile range, the black diamond marker represented the mean value, and the black horizontal line represented the median value in the box plots.

~~Fig. 6 The scatter plots of (a) NCs of the aerosol accumulation mode and WS, (b) NCs of the aerosol coarse mode and WS. The observation data were binned to the WS intervals equal to 3 m s^{-1}; the boxes represented the 25th to 75th percentile value, the black whisker represented the 1.5 inter-quartile range, the black diamond marker represented the mean value, and the black horizontal line represented the median value in the box plots.~~

Fig. 6 (a) The 72-h backward trajectory air mass source traces in the offshore (red solid lines) and pelagic (blue solid lines) regions. (b) Detailed map of the backward trajectory air mass source traces passing through the mainland areas (© Google Earth).

Fig. 7 Classification of the shipboard observation path in the SCS: (a) Accumulation and coarse mode particle sizes graded NCs in the offshore and pelagic regions. For the box plots, the boxes represented the 25th to 75th percentile value, the black whisker represented the maximum and minimum range, the black triangle represented the 1.5 inter-quartile range, the black diamond marker represented the mean value, and the black horizontal line represented the median value. (b) The NCs of average size distributions (the solid lines and circles) and standard deviations (the shaded areas) for marine aerosols of 0.5 to 10 μm diameters in the offshore and pelagic regions. (c) The daily average variations of the proportions and the NCs of two aerosol particle modes were shown with the distances from coast. (d) The distributions of marine aerosol components in the offshore and pelagic regions. The pie charts showed the average aerosol composition based on the mass concentrations from the Merra-2 aerosol dataset during the whole cruise period.

~~Fig. 7 Classification of the shipboard observation path in the SCS: (a) Accumulation and coarse mode particle sizes graded NCs in the offshore and pelagic regions. For the box plots, the boxes represented the 25th to 75th percentile value, the black whisker represented the maximum and minimum range, the black triangle represented the 1.5 inter-quartile range, the black diamond marker represented the mean value, and the black horizontal line represented the median value. (b) The NCs of average size distributions (the solid lines and circles) and standard deviations (the shaded areas) for marine aerosols of 0.5 to 10 μm diameters in the offshore and pelagic regions. (c) The diurnal variations of the proportions and the NCs of two aerosol particle modes were shown with the distances from the coast. (d) The distributions of marine aerosol components in the offshore and pelagic regions. The pie charts showed the average aerosol composition based on the mass concentrations from the Merra-2 aerosol dataset during the whole cruise period.~~

~~Fig. 8 (a) The 72-h backward trajectory air mass source traces in the offshore (orange solid lines) and pelagic (blue solid lines) regions. (b) Detailed map of the backward trajectory air mass source traces passing through the mainland areas (© Google Earth).~~

Fig. ~~9~~8 (a) Diurnal variations of the total mean values of the NCs in the different aerosol particle modes. The vertical bars showed the standard errors (the shadow areas represented the transition periods between daytime and nighttime). (b) The NCs of average size distributions for marine aerosols of 0.5 to 10 μm diameters in different time periods. (c) The NCs of the different aerosol particle modes in different time periods. For the box plots, the boxes represented the 25th to 75th percentile value, the black whisker represented the maximum and minimum range, the black triangle represented the 1.5 inter-quartile range, the black diamond marker represented the mean value, and the black horizontal line represented the median value.

Fig. ~~10~~9 (a) The correlation coefficients between the NCs of all aerosol particle modes and different meteorological parameters. Correlation plot showing the Pearson correlation values of all marine aerosol NCs and meteorological parameters measured in pelagic regions. (b) The comparisons between the diurnal variations of ~~total~~total NCs, SST, SST-T_{2m}, and WS.

Fig. ~~11~~10 The NCs versus WS in the pelagic region. The NC of all aerosol particle modes versus WS for 28-29 °C (a), 29-30 °C (b), and 30-31 °C (c) SST intervals. The error bars represented the standard deviations. The R represented the Pearson correlation coefficients, and the p values were performed to test whether the correlations were significant.

~~Fig. 12 The NCs versus SST in the pelagic region. The NC of all aerosol particle modes versus SST for 0-3 m s^{-1} (a), 3-6 m s^{-1} (b), 6-9 m s^{-1} (c), 9-12 m s^{-1} (d), and 12-15 m s^{-1} (e) WS intervals. The error bars represented the standard deviations. The R represented the Pearson correlation coefficients, and the p values were performed to test whether the correlations were significant.~~

Fig. ~~13~~11 The relationship between the NC of all aerosol particle modes and WS (a), SST (b), and SST-T_{2m} (c). The error bars represented the standard deviations. The R represented the Pearson correlation coefficients, and the p values were performed to test whether the correlations were significant.

~~Fig. 14 The NCs versus SST-T_{2m} in the pelagic region. The NC of all aerosol particle modes versus SST-T_{2m} for 0-3 m s^{-1} (a), 3-6 m s^{-1} (b), 6-9 m s^{-1} (c), 9-12 m s^{-1} (d), and 12-15 m s^{-1} (e) WS intervals. The error bars represented the standard deviations. The R represented the Pearson correlation coefficients, and the p values were performed to test whether the correlations were significant.~~

~~Fig. 15 The NCs versus SST-T_{2m} in the pelagic region. The NC of all aerosol particle modes versus SST-T_{2m} for 28-29 °C (a), 29-30 °C (b), and 30-31 °C (c) SST intervals. The error bars represented the standard deviations. The R represented the Pearson correlation coefficients, and the p values were performed to test whether the correlations were significant.~~